Aus der Neurologischen Universitätsklinik Tübingen
Abteilung Neurologie mit Schwerpunkt neurovaskuläre Erkrankungen

The role of endogenous μ-oscillatory phase in corticospinal excitability and interhemispheric communication between the primary motor cortices assessed by real-time electroencephalography-triggered transcranial magnetic stimulation

Inaugural-Dissertation
zur Erlangung des Doktorgrades
der Medizin

der Medizinischen Fakultät
der Eberhard Karls Universität
zu Tübingen

vorgelegt von

Stefanou, Maria-Ioanna

2021

Dekan:	Professor Dr. B. Pichler
1. Berichterstatter	Professor Dr. U. Ziemann
2. Berichterstatter:	Professor Dr. J. Born
3. Berichterstatter:	Professorin Dr. D. Saur
Tag der Disputation:	28.06.2021

Acknowledgements

I would like to thank Professor Ziemann for including me in his research team and offering me the opportunity to work on this project.

I am also deeply grateful to all the members of the Brain Networks and Plasticity Lab for their guidance, support and encouragement throughout the course of this project.

Table of contents

1. Introduction

The primary motor cortex (M1), with its direct projections to spinal motoneurons, holds a crucial role in dexterous, voluntary limb movement (Yokoi et al., 2018, Rathelot and Strick, 2009). In monkey motor cortex, electrophysiological studies implementing neural recordings have demonstrated that movement-related M1 neuronal firing (i.e., before or during motor tasks) occurs in conjunction with movement both of the contra- and ipsilateral upper limb (Lecas et al., 1986, Georgopoulos et al., 1988). Within the motor network, interhemispheric interactions between the two M1 subserve lateralization of brain functions, suppression of "mirror movements" (Hubers et al., 2008), but also interhemispheric integration and coordinated bimanual movement (van der Knaap and van der Ham, 2011).

Anatomically, the corpus callosum is an essential conveyor of interhemispheric M1-M1 communication (van der Knaap and van der Ham, 2011). Transcallosal communication has been shown to be predominantly mediated by excitatory axons, which cross the corpus callosum to act on local inhibitory neurons in the contralateral motor cortex (Daskalakis et al., 2002). Further inter-regional, cortico-cortical, subcortical and afferent pathways to the primary motor areas form the structural substrate of M1-M1 interactions (Reis et al., 2008).

Within the motor network, interhemispheric interactions between the two M1 are thought to dynamically fluctuate between inhibitory and excitatory functional states, as reflected in the well-studied electrophysiological phenomena of interhemispheric inhibition (Ferbert et al., 1992) and facilitation (Ugawa et al., 1993). From a functional perspective, interhemispheric communication – both within but also outside the motor system - has been shown to be entrained in ongoing oscillations of reciprocal neural assemblies (Engel et al., 1991, Murthy and Fetz, 1996). Studies in cat visual cortex, for example, have indicated that interhemispheric oscillatory synchronization between homologous cortical areas is crucial for the binding of distributed features of neural information (Engel et al., 1991), while in humans, long-distance, interhemispheric neuronal synchronicity has been demonstrated in the beta (13–30 Hz) and gamma (25–40 Hz) bands, during cognitive tasks (Rodriguez et al., 1999, Varela et al., 2001, Fries, 2005, Fries, 2015, Womelsdorf and Fries, 2006). The temporal binding through neural synchrony has been shown to occur with a precision in the millisecond range and has been implicated in conscious processing, arousal,

perceptual integration, attentional selection and working memory (Engel and Singer, 2001). This growing line of evidence on cortico-cortical communication through transient synchronization of neuronal oscillations has led to the formulation of the theory of "neuronal communication through coherence" (Fries, 2005, Fries, 2015).

In the somatosensory cortex, interhemispheric M1-M1 interactions have been studied in behaving non-human primates using bilateral recordings of local field potentials (LFP) (Murthy and Fetz, 1996). These studies show that gamma band oscillations occur simultaneously at bilateral sites - within the left and right M1- for unimanual and bimanual movements (Murthy and Fetz, 1996). Notably, these LFP oscillations at reciprocal M1 cortical areas appear transiently synchronized with negligible phase shifts (Murthy and Fetz, 1996).

Although task-related interhemispheric M1-M1 interactions engage mostly beta and gamma-band oscillations, recent experimental findings from resting-state electroencephalography (EEG) and magnetoencephalography (MEG) recordings have associated interhemispheric, alpha-band (8–12 Hz) synchronization with movement performance and motor control (Dubovik et al., 2012). Studies in stroke patients also indicate that alpha-connectivity (indexed by resting-state alpha-band coherence), between critical nodes of the motor circuitries of the ipsi- and contra-lesional hemispheres, is significantly associated with neuronal plasticity and motor outcome after stroke (Westlake et al., 2012, Nicolo et al., 2015, Dubovik et al., 2012). Moreover, in the healthy human somatosensory cortex, alpha-band inter-regional phase-coupled oscillations have been found to mediate behavioral performance and somatosensory perception (Haegens et al., 2011a, Mima et al., 2001).

At rest, μ-oscillations in the alpha-band constitute the most prominent rhythm in the frequency spectrum of the sensorimotor cortex (Palva and Palva, 2007). Despite being previously considered to reflect cortical idling (Pfurtscheller et al., 1996), μ-rhythm is currently regarded as an active inhibitory mechanism, gating neural processing (Haegens et al., 2011a), while the phase of μ-oscillation is thought to correspond to cyclic excitability changes in the sensorimotor cortex (Klimesch et al., 2007, Berger et al., 2014). Thus, converging evidence supports the view that different phases of endogenous μ-oscillations influence corticospinal excitability (Haegens et al., 2011b, Zrenner et al., 2018b, Berger et al., 2014), as well as large-scale network communication within the human sensorimotor system (Palva and Palva, 2007, Haegens et al., 2011a). Here, we focus on the role of μ-oscillations in the primary motor cortex at rest and examine the role of endogenous μ-oscillations in interhemispheric communication between the human primary motor cortices.

2. Rationale and structure of the thesis

In the present thesis, we were concerned with the role of endogenous phase of sensorimotor μ-rhythm in modulating corticospinal excitability and interhemispheric M1-M1 communication. To this end, we used a millisecond-resolution EEG-triggered transcranial magnetic stimulation (TMS) system, which synchronizes TMS with specific phases of ongoing μ-oscillations over the two sensorimotor cortices (see below). TMS evokes action potentials in human cortex with a spatiotemporal precision of millimeters and milliseconds (Hallett, 2007). Thus, TMS comprises a unique research modality in that it facilitates specific interaction with ongoing network dynamics of the human brain, at a mesoscopic scale, and enables highly precisely non-invasive studies of the temporal dynamics of neuronal network communication (Mueller et al., 2014).

In the first part of this thesis, we present a custom millisecond-resolution EEG-triggered TMS system and the methodology of brain-state-dependent EEG-TMS, which was used for all subsequent experiments (Zrenner et al., 2018a). Synchronized TMS pulses were delivered herein within predetermined EEG-derived phases of the ongoing μ-oscillations to the human primary motor cortex, using motor evoked potentials (MEP) as measure of corticospinal excitability (Stefanou et al., 2019). Using the same brain-state-dependent EEG-triggered TMS technique as in previous studies (Zrenner et al., 2018a), we show that the negative EEG deflection of the μ-rhythm corresponds to a higher cortical excitability state (leading to larger MEP amplitudes) as compared to the positive EEG deflection. In this methodological paper (Stefanou et al., 2019), we also show that utilization of real-time EEG-TMS may reduce inter-trial variability of the TMS-induced corticospinal excitability effects, and we elaborate on the methodological challenges and future potentials of EEG-TMS research.

In the second part of the thesis, we are concerned with the question of symmetry of μ-rhythm phase-dependency of corticospinal excitability between the two M1 (Stefanou et al., 2020). Based on extensive functional and structural interhemispheric asymmetries between homologous areas in the M1 cortices (i.e., between the hand-representation areas of the dominant vs. non-dominant M1) (Amunts et al., 2000), we hypothesized that differences in the μ-phase dependency of corticospinal excitability (e.g., in directionality or effect size) might be noted. Our aim was to assess whether the μ-oscillation phase-dependency of corticospinal excitability may be regarded as a ubiquitous physiological trait of the motor system at rest or, alternatively, shows hemispheric

asymmetry (Stefanou et al., 2020). To address this question, we applied single-pulse TMS to the hand representation areas of both M1 when EEG indicated certain pre-stimulus μ-rhythm phases (i.e., positive peak, negative peak, or random). We then assessed possible asymmetries in the directionality or effect size of μ-phase dependency of corticospinal excitability in the two M1. The study results are presented in the second paper of this thesis (Stefanou et al., 2020).

In the third part of the thesis, we are concerned with the role of endogenous phase of sensorimotor μ-rhythm in interhemispheric M1-M1 communication. With respect to interhemispheric M1-M1 interactions, the interhemispheric inhibition comprises a well-studied phenomenon, which can be measured using paired-pulse TMS by applying a conditioning stimulus (CS) over one primary motor cortex, followed by a second test stimulus (TS) after a short inter-stimulus interval (ISI) over the contralateral motor cortex (Ferbert et al., 1992, Daskalakis et al., 2002). With respect to ISI duration, the application of CS has been shown to lead to attenuation of the size of the test MEP, when CS precedes the TS by an ISI of 5 to 50 ms (Daskalakis et al., 2002). This type of short-interval interhemispheric inhibition (sIHI) has been acknowledged as a stable electrophysiological phenomenon (i.e., thereby suitable as measure of interhemispheric communication), with high reproducibility in animal studies, where stimulation of one motor cortex has been shown to inhibit the contralateral motor cortex for a period of several milliseconds (Chang, 1953, Asanuma and Okuda, 1962).

In the third paper of this thesis (Stefanou et al., 2018), we used sIHI as a measure of effective interhemispheric connectivity between the conditioning and the test M1 and performed an EEG-triggered paired-pulse TMS study to assess the effects of pre-stimulus phase of μ-rhythm on interhemispheric M1-M1 communication. Based on our previous findings that the EEG-negative peak of the endogenous sensorimotor μ-rhythm corresponds to a high-excitability state of the sensorimotor cortex (Zrenner et al., 2018b), and in accordance with the theory of communication through coherence (Fries, 2005, Fries, 2015), we hypothesized that when both M1 were at a high-excitability state (i.e., in-phase negative-peak condition) interhemispheric communication would be most efficient. Thus, we assumed that strongest sIHI would be noted when both the conditioning and the test M1 were stimulated in their high-excitability state (corresponding to the EEG-negative μ-rhythm peak). These study results are presented in the third paper of this thesis (Stefanou et al., 2018).

jove Journal of Visualized Experiments www.jove.com

Video Article

Brain State-dependent Brain Stimulation with Real-time Electroencephalography-Triggered Transcranial Magnetic Stimulation

Maria-Ioanna Stefanou[1,2], David Baur[1,2], Paolo Belardinelli[1,2], Til Ole Bergmann[1,2], Corinna Blum[1,2], Pedro Caldana Gordon[1,2], Jaakko O. Nieminen[1,2,3], Brigitte Zrenner[1,2], Ulf Ziemann[1,2], Christoph Zrenner[1,2]

[1]Department of Neurology & Stroke, University of Tübingen

[2]Hertie Institute for Clinical Brain Research, University of Tübingen

[3]Department of Neuroscience and Biomedical Engineering, Aalto University

Correspondence to: Ulf Ziemann at ulf.ziemann@uni-tuebingen.de

URL: https://www.jove.com/video/59711
DOI: doi:10.3791/59711

Keywords: Behavior, Issue 150, real-time, brain state-dependent stimulation, EEG-TMS, corticospinal excitability, motor cortex, human brain plasticity, phase, oscillation

Date Published: 8/20/2019

Citation: Stefanou, M.I., Baur, D., Belardinelli, P., Bergmann, T.O., Blum, C., Gordon, P.C., Nieminen, J.O., Zrenner, B., Ziemann, U., Zrenner, C. Brain State-dependent Brain Stimulation with Real-time Electroencephalography-Triggered Transcranial Magnetic Stimulation. *J. Vis. Exp.* (150), e59711, doi:10.3791/59711 (2019).

Abstract

The effect of a stimulus to the brain depends not only on the parameters of the stimulus but also on the dynamics of brain activity at the time of the stimulation. The combination of electroencephalography (EEG) and transcranial magnetic stimulation (TMS) in a real-time brain state-dependent stimulation system allows the study of relations of dynamics of brain activity, cortical excitability, and plasticity induction. Here, we demonstrate a newly developed method to synchronize the timing of brain stimulation with the phase of ongoing EEG oscillations using a real-time data analysis system. This real-time EEG-triggered TMS of the human motor cortex, when TMS is synchronized with the surface EEG negative peak of the sensorimotor μ-alpha (8-14 Hz) rhythm, has shown differential corticospinal excitability and plasticity effects. The utilization of this method suggests that real-time information about the instantaneous brain state can be used for efficacious plasticity induction. Additionally, this approach enables personalized EEG-synchronized brain stimulation which may lead to the development of more effective therapeutic brain stimulation protocols.

Video Link

The video component of this article can be found at https://www.jove.com/video/59711/

Introduction

TMS is a well-established method for noninvasive brain stimulation and enables the specific modulation of ongoing network dynamics and studies of corticocortical and corticospinal neural pathways with high spatiotemporal precision[1]. When stimulating the primary motor cortex (M1), the neural response can be quantified as motor evoked potentials (MEPs), as well as TMS-evoked EEG potentials. MEPs can be recorded by electromyography (EMG) of target muscles, and their amplitude reflects corticospinal excitability when stimulating the primary motor cortex[2].

Despite the unique potential of noninvasive brain stimulation as a scientific tool to investigate and modulate brain networks in healthy study participants and in patients, TMS studies suffer from large trial-to-trial and intra- and interindividual variability of evoked responses[3,4,5]. Specifically, in TMS studies of corticospinal excitability and plasticity, MEP responses, as well as induced long-term potentiation (LTP)- or long-term depression (LTD)-like plasticity, exhibit high intrinsic variability, even when the stimulus parameters are carefully controlled[3,4]. However, evidence from animal studies indicates that the observed variability of responses is not attributable to "random noise" but is instead related to the fluctuating brain states at the time of stimulation[6]. Accordingly, by combining TMS with EEG in a real-time brain-state-dependent stimulation paradigm (i.e., EEG-triggered TMS), the fluctuating instantaneous brain state can be used to optimize stimulus timing[7,8,9,10].

Several studies have related the instantaneous phase of ongoing neural oscillations to neuronal excitability using TMS-compatible EEG systems[11,12]. Modern EEG amplifiers can handle the large electromagnetic TMS artifacts, and increasingly well-established experimental protocols exist for the combination of EEG with TMS[13,14] and the post hoc removal of TMS-related EEG artifacts[15,16]. While the influence of the prestimulus brain state as assessed by EEG on TMS-evoked responses can be assessed with randomly applied TMS stimuli that are sorted post hoc[17,18], the repetitive application of TMS in a predefined brain state requires real-time EEG-triggered TMS[11,19].

Here, a custom millisecond-resolution EEG-triggered TMS setup is used to synchronize TMS pulses with a predetermined phase of ongoing brain oscillations[11], demonstrating that the negative EEG deflection of the μ-alpha rhythm corresponds to a higher cortical excitability state (leading to larger MEP amplitudes) as compared to the positive EEG deflection[8,11,12,20]. In this manuscript, we present a method for conducting real-time EEG-triggered TMS protocols to study human brain networks.

Protocol

All experimental procedures described in the following sections have been approved by the Institutional Ethics Committee following the guidelines of the Declaration of Helsinki, and all participants provided written informed consent prior to study enrollment.

1. Study Participants

1. **Subject recruitment**
    1. Recruit study participants based on predefined inclusion criteria. Screen candidates for contraindications, such as the presence of implanted medical devices (e.g., cardiac pacemaker), according to TMS safety guidelines[21], or for neurological or psychiatric diseases and the use of drugs that act on the nervous system.
    2. For studies requiring magnetic resonance imaging (MRI), assess the potential study participants for possible contraindications to MRI according to radiological safety standards[22]. Perform a power analysis to ensure that the study sample is sufficient for statistical analysis.
    3. Optionally, preselect subjects having a prominent oscillation of interest in the signal extracted by the chosen EEG montage in order to improve the accuracy of the phase detection.
    NOTE: In this experiment, the C3-centered Laplacian (C3 referenced to the average of the surrounding electrodes CP1, CP5, FC1, and FC5) was used to extract the sensorimotor μ-rhythm with the subject at rest and eyes open. Preselected were subjects having a single peak in the alpha band (8-14 Hz) which contains >25% of total power in the current source density (CSD) power spectrum. This criterion ensured that the oscillation amplitude was sufficiently large in comparison to the background noise (good signal-to-noise ratio [SNR]) to enable the algorithm to estimate the instantaneous phase of the trigger signal with sufficient accuracy and increased the likelihood of observing a significant excitability effect[11,12,28,29,30].

2. **Subject information**
    1. Provide the subjects with the study-related informed consent form. Provide printed TMS and MRI safety screening questionnaires.
    NOTE: These documents and the study protocol, as well as the use of personal data (e.g., from questionnaires) and identifiable human data (e.g., from MRI), need to be preapproved by the ethics committee (Institutional Review Board).
    2. Ask the subject to fill out the TMS and MRI safety screening questionnaires. Acquire written informed consent for participation in the study and the planned use of data.
    3. Acquire demographic data.
    4. Assess subject handedness using standard inventories (e.g., the Edinburgh Handedness Inventory)[23].
    5. Introduce the subject to the setup and stimulation procedure. Ensure that each participant is familiarized with the sensation of TMS and tolerates it well.
    6. Acquire MRI for each participant prior to the TMS experimental sessions. Whole-head anatomical MR images are required, including the top of the scalp and anatomical landmarks (i.e., the tragus of both ears), as these will serve as fiducial points for neuronavigation in subsequent steps of this protocol.
    7. Schedule the experimental sessions according to the specifications of the study protocol (i.e., take into account "washout periods" between the experiments).
    NOTE: Ideally, subjects should come at the same time and on the same day of the week in protocols comparing different conditions in multiple sessions.
    8. Instruct the participants to refrain from consuming alcohol, nicotine, or caffeine before the scheduled experimental sessions. The subjects should also have had their regular sleep on the night before the experiment and not be unusually tired.

2. Setup Preparation

1. **Real-time-data-stream-capable EEG system**
    1. Use a TMS-compatible EEG/EMG amplifier that can handle the voltage spikes induced by the TMS pulse.
    NOTE: The amplifier system needs to make a raw data stream available at a constant low latency (<5 ms) for subsequent processing by a real-time processor. In this experiment, a 24-bit 80-channel biosignal amplifier was used for EEG and EMG recordings.
    2. Configure the EEG/EMG amplifier system to low-pass filter (e.g., 0.16 Hz cut-off), and down-sample the biosignal data to 5 kHz from the sampling rate at the amplifier head stage.
    3. Ensure that the amplifier system sends data packets containing the relevant channels via a real-time user datagram protocol (UDP) to the real-time processor at regular constant intervals ≤1ms. Use a high sampling frequency (e.g., 5 kHz) to capture the EMG responses and to minimize filter delay of the EEG data.

2. **EEG-compatible TMS device**
    1. Use a TMS device that can be triggered externally with a fixed and minimal delay and which minimizes artifacts in the simultaneous EEG recording (e.g., line noise in the EEG through the TMS coil cable, recharging artifacts after the pulse).
    2. Ensure that the distance between the TMS stimulator (including the coil and coil cable) and the EEG recording system is maximized to reduce electrical interference (at least 1 m). Where possible, turn off sources of electromagnetic interference such as fans and motors. Furthermore, ensure that the EEG and EMG recording leads are positioned and aligned such that common interference cancels out.

3. **Real-time EEG data processing system**
NOTE: The real-time EEG data stream is acquired and analyzed using a real-time digital signal processing system, which then triggers the TMS device when a predetermined condition is met. Such a system has been custom-developed in our laboratory[11] to implement a phase detection algorithm similar to the approach by Chen et al.[24] and consists of the following steps.

1. Analyze a sliding window of data, 500 ms long (**Figure 1a**), to estimate the instantaneous phase of the target brain oscillation to phase-specifically trigger the TMS stimulator.
2. Perform bandpass filtering of the window for the frequencies of interest (e.g., between 9 and 14 Hz for the sensorimotor μ-alpha rhythm; **Figure 1b**). Consider adjusting the filter parameters to the individual peak frequency of the target oscillation.
3. Remove any data distorted by the filtering edge effects. Note that there is a trade-off in that stronger filters have larger edge effects.
4. Use an autoregressive model to forward predict the signal (Yule-Walker, order 30; **Figure 1c**).
5. Apply a Hilbert transform of the resulting window of data to yield the analytic signal, from which the instantaneous phase of the signal is determined by taking the angle of the complex number at the relevant time-point.
6. Estimate the EEG power spectrum from the sliding window of data in the frequency bins of interest (e.g., 9-14 Hz) using a short-time Hann-windowed FFT.
7. When both phase and power meet a predetermined criterion (e.g., a negative peak, the minimum power threshold), generate a digital output (TTL) pulse with the real-time system to trigger the TMS device.

4. **Neuronavigation system**
   1. To monitor coil position and achieve accurate and consistent TMS targeting within and across sessions, use a neuronavigation system.
      NOTE: A stereo infrared camera system is used precisely to locate in three-dimensional space reflective trackers, which are mounted on the subject's head and the stimulation coil, enabling precise relative positioning of the coil with respect to the individual's brain anatomy after calibration and MRI registration. For single-session studies and when planning to analyze only the EMG and not the EEG responses to TMS, navigation based on a standard brain instead of an individual MRI is sufficient.
   2. Load the individual structural MRI data into the navigation system software prior to starting the experiment for each participant.

5. **Experimental control computer**
   1. Use an experimental control computer that is connected to the EEG system, the TMS device, the real-time device, and the neuronavigation system.
      NOTE: The EEG software controls the EEG amplifier system, sets parameters, and starts and stops EEG data archiving. The TMS device can be remote-controlled to change stimulation parameters (intensity, current direction, etc.) with a remote-control toolbox[25].
   2. Remotely control the real-time device to set the desired trigger conditions.
      NOTE: The neuronavigation system can be remote-controlled, for example to target different coil locations.
   3. Combine all of the above in an experimental control script to enable the automation of the experimental conditions and control flow.

6. **EEG recording electrodes**
   1. Ensure that TMS-compatible EEG recording caps with the desired electrode layout are available in different sizes. Measure the subject's head circumference and prepare the appropriately sized cap.
   2. Keep the required materials for EEG preparation handy (e.g., abrasive and conductive gels, syringes with sterile blunt needles, etc.).

7. **EMG recording electrodes**
   1. Keep the surface EMG electrodes, leads, and required materials for skin preparation ready.

3. Conducting the Experiment

1. **Preliminaries**
   1. Ensure that the required paperwork is in order (study consent form is signed) and that the participant has had no adverse effects since the previous session.
   2. Seat the subject in a comfortable reclining position to minimize movement of the head during the experiment. A vacuum pillow wrapped around the neck and lower head can help to support the participant's head without causing additional muscle tension (e.g., like a chin rest would do).

2. **EEG and EMG preparation**
   1. Place the appropriately sized EEG cap on the subject's head and position the cap correctly. Avoid excessive tension below the chin to reduce cranial and neck muscle activity that could contaminate the EEG[26].
   2. Register the subject in the EEG recording software.
   3. Prepare the EEG electrodes according to the lab-specific protocol (e.g., apply abrasive gel followed by conductive gel).
   4. Check that EEG electrode impedances are below 5 kΩ.
   5. To keep the conducting gel from drying up or getting smeared to the adjacent electrodes by any movement of the TMS coil, cover the EEG cap with plastic wrap. Then, fit a net cap above the plastic wrap to keep the cables in a fixed position to reduce EEG-artifact variability, and apply adhesive tape to increase the stability of the multiple layers.
   6. Attach the surface EMG electrodes over the target muscles after having cleaned and lightly abraded the skin (e.g., use a bipolar recording from the right abductor pollicis brevis hand muscle in a belly-tendon montage).
      NOTE: Here, a bipolar recording from the right abductor pollicis brevis hand muscle in a belly-tendon montage was used. The placement of EMG electrodes is important as surface electrodes generally record activity from multiple underlying muscles.
   7. Verify the correct matching between the actual EEG sensors on the head and the traces recorded in the EEG system by tapping on a few EEG electrodes to cause artifacts. As a sanity check, verify that occipital alpha increases when the participant closes their eyes.
   8. Visually inspect the ongoing EEG and EMG signal for artifacts (e.g., line noise, muscle activity) or bad electrodes.
   9. Ensure that the participant remains awake and keeps their eyes open throughout the experiment to avoid occipital alpha oscillations contaminating the signal.

3. **Preparation of the neuronavigation**
   1. Attach the reflective head tracker to the participant's head with sufficient adhesive tape to ensure stability throughout the experiment.

2. Use the pointer tool to coregister the head model with the relevant anatomical landmarks (e.g. the nasion, the tragi of both ears, the corners of the eyes).
3. Attach a coil tracker to the stimulation coil and calibrate the coil.
4. Place the pointer at different points on the head surface and verify the correctness of the displayed position on the monitor of the neuronavigation system.
5. Pinpoint the EEG sensor locations for coregistration with the individual MRI.

4. **Baseline EEG**
   1. Demonstrate typical EEG artifacts to the subject (e.g., swallowing, chewing, eye blinks) and instruct the subject to avoid them throughout the experiment. Also, ask them to avoid jaw clenching, yawning, or talking.
   2. Ask the subject to fixate on a point with the eyes open and perform a short recording of resting-state EEG with the eyes open.
   3. If required for the computation of real-time filters, record additional EEG activity during tasks.

5. **Finding the motor "hotspot" and determination of the resting motor threshold**
   1. Find the motor "hotspot" (i.e. the stimulation location over which single-pulse TMS elicits well-shaped MEPs of a comparably consistent amplitude across trials) and save the corresponding coil position (including coil orientation and angulation) in the neuronavigation system.
   2. Find the resting motor threshold (RMT) by applying single TMS pulses over the motor cortex at gradually increasing stimulation intensities until the elicited MEPs have peak-to-peak amplitudes greater than 50 µV in more than 50% of the trials[21].
   3. If available, use an automated script for parameter estimation by sequential testing (PEST), for instance, following a maximum likelihood strategy[27] which also provides an online estimate of the confidence interval of RMT based on the observed variability of single responses and which typically requires ca. 30 test pulses of adaptively varying intensity to obtain a robust RMT estimate.
   4. If this is not the first experimental session, compare the coil position with the previous position and compare the obtained RMT with the previous RMT to validate consistency.
   5. If required, determine stimulation intensities for the active motor threshold (AMT) or for the 1-mV peak-to-peak MEP amplitude using standard procedures[21].

6. **Final participant preparation**
   1. Optionally, immobilize the head of the subject using a vacuum pillow.
   2. Optionally, deliver a masking noise through earplugs (when planning to analyze TMS-evoked EEG potentials). Otherwise, provide the subject with earplugs and headphones for hearing protection.
   3. Optionally, align and fix the coil at the desired position using a mechanical arm.

7. **Pre-experiment data quality validation**
   1. Check that the real-time processor is receiving data from the EEG system.
   2. Check the signal obtained from the desired EEG spatial filter (e.g., C3-centered Laplacian montage) for obvious artifacts.
   3. Visually confirm the EEG signal quality, check for bad electrodes, excessive line noise, and muscle artifacts, and adjust the time window and amplitude scaling on the EEG system software for ongoing visual inspection during the experiment.

8. **Main experimental session**
   1. Unless the stimulator intensity is remote-controlled in the experimental script, manually set the stimulation intensity to the desired value (e.g., 110% of the RMT).
   2. Start the experimental script to apply pulses at different phases of the target oscillation in a randomized order.
   3. During the experiment, monitor the trigger condition thresholds (artifact-detection threshold, pre-innervation threshold, minimum power, etc.).
      NOTE: Stimuli will be triggered at irregular intervals, as the real-time processor is waiting for the trigger conditions to occur. However, the conditions should be set such that most stimuli occur within a predictable interval (e.g., 2-3 s after the previous pulse), and long pauses (e.g., in this case, >5 s) are avoided as these would lead to larger evoked responses due to novelty.
      1. Alternatively, use post hoc stratification to remove trials following overly long intervals.
   4. To achieve sufficient statistical power to differentiate phase-specific stimulation effects, acquire a sufficient number of trials
      NOTE: We typically chose 80-120 interleaved trials per condition[20].
   5. Document the start and end times of the various sessions and keep a record of any unusual occurrences.

Representative Results

The utilization of the real-time EEG-triggered TMS in the human primary motor cortex reveals differential corticospinal excitability and plasticity effects. Using the protocol described above, real-time EEG-TMS was applied, synchronizing TMS with the ongoing EEG oscillatory phase of the endogenous sensorimotor µ-rhythm in three trigger conditions (positive peak, negative peak, and random phase) in randomized order. A Laplacian EEG montage was used to extract the sensorimotor µ-rhythm by referencing the EEG electrode C3 to the average of four surrounding electrodes (FC1, FC5, CP1, and CP5). **Figure 2a** shows the average prestimulus EEG signal in the 400 ms before the TMS pulse for the three predefined conditions. The average elicited MEPs recorded from the right-hand muscles are depicted in **Figure 2b**. These results show that the negative EEG deflection of the µ-rhythm corresponds to a higher cortical excitability state (leading to larger MEP amplitudes) as compared to the positive EEG deflection, with low intertrial variability of the noted corticospinal excitability effects, presented in **Figure 2c**.

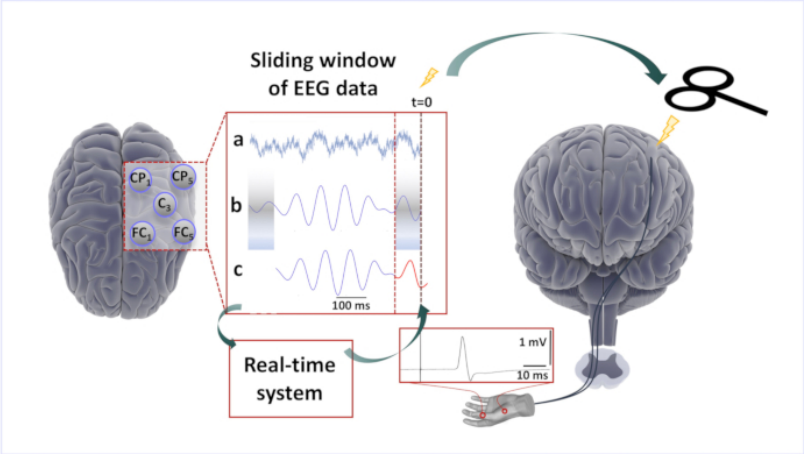

Figure 1: Brain-state-dependent EEG-phase-triggered TMS. Scalp EEG raw data derived from a five channel Laplacian montage centered on the C3 electrode over the left sensorimotor cortex was acquired sample-by-sample by a real-time digital signal processing system. (**a**) A 500-ms sliding window of EEG data was processed by the algorithm every 2 ms. (**b**) The signal after band-pass filtering and removal of the edge artifacts. (**c**) The forward-predicted signal (red trace) based on an autoregressive forecasting model that was calculated from the window of data. The phase at time zero ("right now") was estimated using a Hilbert transform, the spectral power was estimated from the window of data. The TMS stimulator was triggered when a predefined phase and spectral amplitude condition were met. TMS over the left primary motor cortex resulted in MEPs in right-hand muscles recorded with surface EMG. Please click here to view a larger version of this figure.

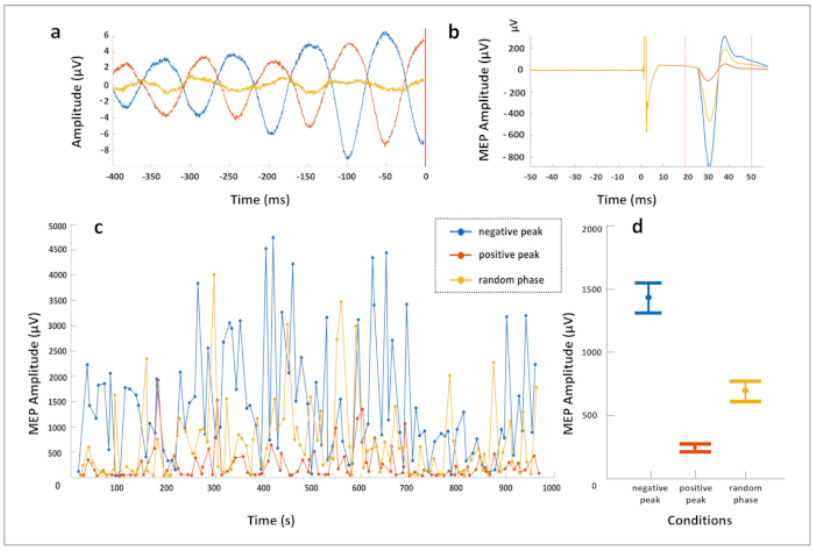

Figure 2: Data from one exemplary subject who received real-time EEG-triggered TMS over the left M1, targeting the phase of the 10 Hz sensorimotor μ-rhythm. A hundred stimuli each were applied according to three phase-trigger conditions (positive peak, negative peak, and random phase) in combination with a constant minimum 10 Hz spectral power threshold condition, in randomized order, with an intertrial interval of approximately 3 s. A Laplacian EEG montage was used to extract the sensorimotor μ-rhythm by referencing the EEG electrode C3 to the average of four surrounding electrodes (FC1, FC5, CP1, and CP5). (**a**) Average prestimulus EEG signal in the 400 ms before the TMS pulse for the three conditions. (**b**) Average EMG trace of the motor evoked potential (MEP) recorded from the right abductor pollicis brevis muscle for each condition. (**c**) Peak-to-peak MEP amplitude (in microvolts) of each trial over time, per trigger condition. Note that the MEPs are largest in the negative peak condition, smallest in the positive peak condition, and intermediate in the random phase condition. (**d**) The mean MEP amplitude in each condition is shown with error bars illustrating the standard error of the mean. Note that a participant with a particularly clear effect has been selected for illustration purposes and that this effect size is not representative for the group average. Please click here to view a larger version of this figure.

Discussion

Brain-state-dependent EEG-triggered TMS is a novel method with unique perspectives with respect to effectiveness and consistency of the ensuing brain-stimulation effects[8,9,31]. The main advantage of the method is that a functionally relevant endogenous brain state may be specifically targeted to trigger the TMS pulse, inducing potentially less variable and longer-lasting brain responses[11]. Real-time EEG-triggered

repetitive TMS in the negative phase of the sensorimotor μ-rhythm of human M1 (i.e., the state of increased corticospinal excitability, **Figure 2**) induced significantly stronger LTP-like plasticity (a long-term increase of MEP amplitude) compared to brain-state-independent TMS[11,20]. In addition to its scientific utility, the application of real-time EEG-TMS to cortical areas, such as the dorsolateral prefrontal cortex (DLPFC), has the potential to increase the effectiveness of current therapeutic brain stimulation protocols.

In this manuscript, we presented the methodological steps for the implementation of real-time EEG-TMS. Fundamental requirements for the conduction of experiments with this method are, first, the use of a TMS-compatible EEG system with a real-time digital out option and, second, the use of real-time signal processing with the implementation of a phase-detection algorithm[24], which extracts the desired brain rhythm (e.g., sensorimotor μ-rhythm) from the recorded EEG signal using spatial filters (e.g., C3-centered Laplacian filter) and applies stimulation when preselected conditions (i.e., phase and power of the targeted brain rhythm) are met. The performance and accuracy of the algorithm depend strongly on the SNR of the EEG recording[20]. Thus, the EEG preparation steps of the protocol are crucial to achieve a high SNR and ensure accurate triggering of the TMS, and a preselection of participants may need to be considered if the respective target oscillation is not sufficiently observable with EEG in every individual. Furthermore, the use of mechanical support arms for the coils and vacuum pillows to immobilize the participant's head is advisable, in order to minimize artifacts due to the varying pressure of the coil on the electrodes.

Regarding the application of the real-time EEG-TMS method in experimental paradigms, the selection of the brain rhythm of interest may vary. Thus, adjustments of the filtering are advisable to facilitate the identification of the targeted brain activity. Recently, several spatial filtering methods have been proposed to optimally extract a functionally relevant brain state (e.g., in channel space[19], with current source density[13], with local spatial filters[11,28], and with individualized filters using, for example, spatial-spectral decomposition[29]). Yet, so far, no unequivocal method exists to extract from surface EEG signals (sensor space) the real brain-oscillation phase (source space). Future studies that assess the correspondence of surface and source-space signals are warranted to improve the precision of real-time EEG algorithms.

Whereas in this protocol we have focused on the 8-14-Hz sensorimotor μ-rhythm to demonstrate the influence of the instantaneous phase of this oscillation on corticospinal excitability, other oscillations (e.g., beta, theta, or infraslow oscillations) may also play a role. This method can, in principle, be used to target the phase for any oscillation that can be isolated with a sufficient SNR, including multiple superimposed oscillations (e.g., a negative cycle of alpha and a simultaneous positive peak of gamma).

One main limitation of the real-time EEG-TMS experiments is that the spatiotemporal resolution with respect to the brain sources is strongly dependent on artifact occurrence and consistency of the stimulation. Therefore, a critical prerequisite of the protocol is the monitoring of the performance of the algorithm (i.e., ensuring that stimulation occurs upon the detection of neuronal and not artifactual activity throughout the experiment). Furthermore, the utilization of neuronavigation for optimal and consistent positioning of the stimulation coil (especially in experimental paradigms using stimulation sites such as the DLPFC) is helpful for reducing response variability due to variability in coil position. Note also, as a further limitation, that specifically selected and configured EEG/EMG, TMS, and real-time processing devices are required, along with experience in preparing and conducting the experiments in such a way as to minimize external sources of response variability that may mask the effect of instantaneous brain-state.

In conclusion, we demonstrated a standard protocol for conducting real-time EEG-TMS experiments and introduced a novel method for utilizing the endogenous brain states of interest (i.e., preselected phases and power of a targeted endogenous brain oscillation) to trigger brain stimulation. Further research using the real-time EEG-TMS method will allow methodological improvements and facilitate the development of effective protocols for the study and modulation of human brain networks.

Disclosures

C.Z. and P.C.G. are partially funded through an EXIST Transfer of Research grant by the German Federal Ministry for Economic Affairs and Energy (grant 03EFJBW169). C.Z. reports additional employment as a part-time employee of the not-for-profit medical innovation foundation (Stiftung für Medizininnovationen, Tübingen, Germany); a subsidiary of this foundation is producing the real-time processor used in this article (Medical Innovations Incubator GmbH, Tübingen, Germany).

Acknowledgments

C.Z. acknowledges support from the Clinician Scientist Program of the Faculty of Medicine, University of Tübingen. U.Z. acknowledges support from the German Research Foundation (grant ZI 542/7-1). T.O.B. acknowledges support from the German Research Foundation (grant BE 6091/2-1). J.O.N. acknowledges support from the Academy of Finland (Decisions No. 294625 and 306845). The authors acknowledge support by the Open Access Publishing Fund of the University of Tübingen.

References

1. Hallett, M. Transcranial magnetic stimulation: a primer. *Neuron.* **55**(2), 187-199 (2007).
2. Barker, A. T., Jalinous, R., Freeston, I. L. Non-invasive magnetic stimulation of human motor cortex. *Lancet.* **1**(8437), 1106-1107 (1985).
3. López-Alonso, V., Cheeran, B., Río-Rodríguez, D., Fernández-del-Olmo, M. Inter-individual variability in response to non-invasive brain stimulation paradigms. *Brain Stimulation.* **7**(3), 372-380 (2014).
4. Müller-Dahlhaus, J. F., Orekhov, Y., Liu, Y., Ziemann, U. Interindividual variability and age-dependency of motor cortical plasticity induced by paired associative stimulation. *Experimental Brain Research.* **187**(3), 467-475 (2008).
5. Ziemann, U., Siebner, H. R. "Inter-subject and inter-session variability of plasticity induction by non-invasive brain stimulation: Boon or bane? *Brain Stimulation.* **8**(3), 662-663 (2015).
6. Arieli, A., Sterkin, A., Grinvald, A., Aertsen, A. Dynamics of ongoing activity: explanation of the large variability in evoked cortical responses. *Science.* **273**(5283), 1868-1871 (1996).

7. Thut, G., Ives, J. R., Kampmann, F., Pastor, M. A., Pascual-Leone, A. A new device and protocol for combining TMS and online recordings of EEG and evoked potentials. *Journal of Neuroscience Methods.* **141**(2), 207-217 (2005).
8. Zrenner, C., Belardinelli, P., Müller-Dahlhaus, F., Ziemann, U. Closed-loop neuroscience and non-invasive brain stimulation: A tale of two loops. *Frontiers in Cellular Neuroscience.* **10**, 92 (2016).
9. Bergmann, T. O. Brain state-dependent brain stimulation. *Frontiers in Psychology.* **9**, 2108 (2018).
10. Matthews, P. B. C. The effect of firing on the excitability of a model motoneurone and its implications for cortical stimulation. *Journal of Physiology.* **518**(3), 867-882 (1999).
11. Zrenner, C., Desideri, D., Belardinelli, P., Ziemann, U. Real-time EEG-defined excitability states determine efficacy of TMS-induced plasticity in human motor cortex. *Brain Stimulation.* **11**(2), 374-389 (2018).
12. Stefanou, M. I., Desideri, D., Belardinelli, P., Zrenner, C., Ziemann, U. Phase synchronicity of μ-rhythm determines efficacy of interhemispheric communication between human motor cortices. *Journal of Neuroscience.* **38**(49), 10525-10534 (2018).
13. Berger, B., Minarik, T., Liuzzi, G., Hummel, F. C., Sauseng, P. EEG oscillatory phase-dependent markers of corticospinal excitability in the resting brain. *BioMed Research International.* **2014**, 936096 (2014).
14. Keil, J. *et al*. Cortical brain states and corticospinal synchronization influence TMS-evoked motor potentials. *Journal of Neurophysiology.* **111**(3), 513-519 (2014).
15. Rogasch, N. C. *et al.* Analysing concurrent transcranial magnetic stimulation and electroencephalographic data: A review and introduction to the open-source TESA software. *NeuroImage.* **147**, 934-951 (2017).
16. Herring, J. D., Thut, G., Jensen, O., Bergmann, T. O. Attention modulates TMS-locked alpha oscillations in the visual cortex. *Journal of Neuroscience.* **35**(43), 14435-14447 (2015).
17. Romei, V. *et al.* Spontaneous fluctuations in posterior α-band EEG activity reflect variability in excitability of human visual areas. *Cerebral Cortex.* **18**(9), 2010-2018 (2008).
18. Sauseng, P., Klimesch, W., Gerloff, C., Hummel, F. C. Spontaneous locally restricted EEG alpha activity determines cortical excitability in the motor cortex. *Neuropsychologia.* **47**(1), 284-288 (2009).
19. Bergmann, T. O. *et al.* EEG-guided transcranial magnetic stimulation reveals rapid shifts in motor cortical excitability during the human sleep slow oscillation. *Journal of Neuroscience.* **32**(1), 243-253 (2012).
20. Schaworonkow, N., Triesch, J., Ziemann, U., Zrenner, C. EEG-triggered TMS reveals stronger brain state-dependent modulation of motor evoked potentials at weaker stimulation intensities. *Brain Stimulation.* **12**(1), 110-118 (2019).
21. Rossi, S., Hallett, M., Rossini, P. M., Pascual-Leone, A., The Safety of TMS Consensus Group. Safety, ethical considerations, and application guidelines for the use of transcranial magnetic stimulation in clinical practice and research. *Clinical Neurophysiology.* **120**(12), 2008-2039 (2009).
22. Kanal, E. *et al.* ACR guidance document for safe MR practices: 2007. *American Journal of Roentgenology.* **188**(6), 1447-1474 (2007).
23. Oldfield, R. C. The assessment and analysis of handedness: The Edinburgh inventory. *Neuropsychologia.* **9**(1), 97-113 (1971).
24. Chen, L. L., Madhavan, R., Rapoport, B. I., Anderson, W. S. Real-time brain oscillation detection and phase-locked stimulation using autoregressive spectral estimation and time-series forward prediction. *IEEE Transactions on Biomedical Engineering.* **60**(3), 753-762 (2013).
25. Habibollahi Saatlou, F. *et al.* MAGIC: An open-source MATLAB toolbox for external control of transcranial magnetic stimulation devices. *Brain Stimulation.* **11**(5), 1189-1191 (2018).
26. Lioumis, P., Zomorrodi, R., Hadas, I., Daskalakis, Z. J., Blumberger, D. M. Combined transcranial magnetic stimulation and electroencephalography of the dorsolateral prefrontal cortex. *Journal of Visualized Experiments.* (138), e57983 (2018).
27. Mishory, A. *et al.* The maximum-likelihood strategy for determining transcranial magnetic stimulation motor threshold, using parameter estimation by sequential testing is faster than conventional methods with similar precision. *The Journal of ECT.* **20**(3), 160-165 (2004).
28. Thies, M., Zrenner, C., Ziemann, U., Bergmann, T. O. Sensorimotor mu-alpha power is positively related to corticospinal excitability. *Brain Stimulation.* **11**(5), 1119-1122 (2018).
29. Schaworonkow, N. *et al.* μ-Rhythm extracted with personalized EEG filters correlates with corticospinal excitability in real-time phase-triggered EEG-TMS. *Frontiers in Neuroscience.* **12**, 954 (2018).
30. Hjorth, B. An on-line transformation of EEG scalp potentials into orthogonal source derivations. *Electroencephalography and Clinical Neurophysiology.* **39**(5), 526-530 (1975).
31. Bergmann, T. O., Karabanov, A., Hartwigsen, G., Thielscher, A., Siebner, H. R. Combining non-invasive transcranial brain stimulation with neuroimaging and electrophysiology: Current approaches and future perspectives. *NeuroImage.* **140**, 4-19 (2016).

SCIENTIFIC REPORTS
nature research

OPEN

Interhemispheric symmetry of μ-rhythm phase-dependency of corticospinal excitability

Maria-Ioanna Stefanou[1,2], Dragana Galevska[1,2], Christoph Zrenner[1,2], Ulf Ziemann[1,2] ✉ & Jaakko O. Nieminen[1,2,3]

Oscillatory activity in the μ-frequency band (8–13 Hz) determines excitability in sensorimotor cortex. In humans, the primary motor cortex (M1) in the two hemispheres shows significant anatomical, connectional, and electrophysiological differences associated with motor dominance. It is currently unclear whether the μ-oscillation phase effects on corticospinal excitability demonstrated previously for the motor-dominant M1 are also different between motor-dominant and motor-non-dominant M1 or, alternatively, are similar to reflect a ubiquitous physiological trait of the motor system at rest. Here, we applied single-pulse transcranial magnetic stimulation to the hand representations of the motor-dominant and the motor-non-dominant M1 of 51 healthy right-handed volunteers when electroencephalography indicated a certain μ-oscillation phase (positive peak, negative peak, or random). We determined resting motor threshold (RMT) as a marker of corticospinal excitability in the three μ-phase conditions. RMT differed significantly depending on the pre-stimulus phase of the μ-oscillation in both M1, with highest RMT in the positive-peak condition, and lowest RMT in the negative-peak condition. μ-phase-dependency of RMT correlated directly between the two M1, and interhemispheric differences in μ-phase-dependency were absent. In conclusion, μ-phase-dependency of corticospinal excitability appears to be a ubiquitous physiological trait of the motor system at rest, without hemispheric dominance.

The hypothesis that μ-oscillatory activity modulates cortical excitability in the sensorimotor cortex has recently received growing experimental support from electrophysiological studies in primates[1] and humans[2–6]. The ongoing oscillations of motor networks at rest have been shown to resonate at the μ-frequency band (8–13 Hz)[7], while the phase of the μ-rhythm has been related to a periodical transition between high- and low-excitability states in neurons of sensorimotor cortex[1]. In a study based on local field potential (LFP) recordings in the right monkey primary motor cortex (M1), neuronal firing rate was highest during the trough of the μ-oscillation, and lowest during its peak[1].

The development of real-time electroencephalography (EEG)-triggered transcranial magnetic stimulation (TMS) has recently enabled a deterministic probing of the effects of the phase of a pre-stimulus oscillation on corticospinal excitability, as indexed by the motor evoked potential (MEP) amplitude, in the human M1. Using real-time brain-state-dependent TMS, we have shown that the EEG negative peak of the μ-oscillation represents a high-excitability state of corticospinal neurons (i.e., larger MEP amplitudes are elicited when TMS is triggered at the EEG negative peak of the μ-oscillation compared to the EEG positive peak)[2–5]. This effect has been demonstrated separately for the M1 of the motor-dominant[2,3] and the motor-non-dominant[4] hemisphere of right-handed subjects.

Although μ-oscillations are ubiquitously present in the sensorimotor cortex at rest[7,8], significant interhemispheric differences in the frequency and power of μ-oscillations have been reported[9,10]. Electrophysiological studies (including LFP studies in primates[1] and EEG–TMS studies in humans[2–5]) have assessed the effects of the pre-stimulus phase of μ-oscillations on M1 excitability unilaterally. We are unaware of electrophysiological evidence regarding the ubiquity (i.e., symmetry) of μ-phase-dependency of cortical excitability across the motor system (i.e., in homologous motor areas across hemispheres). Given the well-established, functional and structural interhemispheric asymmetries between homologous areas in the M1 cortices[11], differences in the μ-phase-dependency of corticospinal excitability (e.g., in directionality or effect size) might be expected.

[1]Department of Neurology & Stroke, University of Tübingen, Tübingen, Germany. [2]Hertie Institute for Clinical Brain Research, University of Tübingen, Tübingen, Germany. [3]Department of Neuroscience and Biomedical Engineering, Aalto University School of Science, Espoo, Finland. ✉e-mail: ulf.ziemann@uni-tuebingen.de

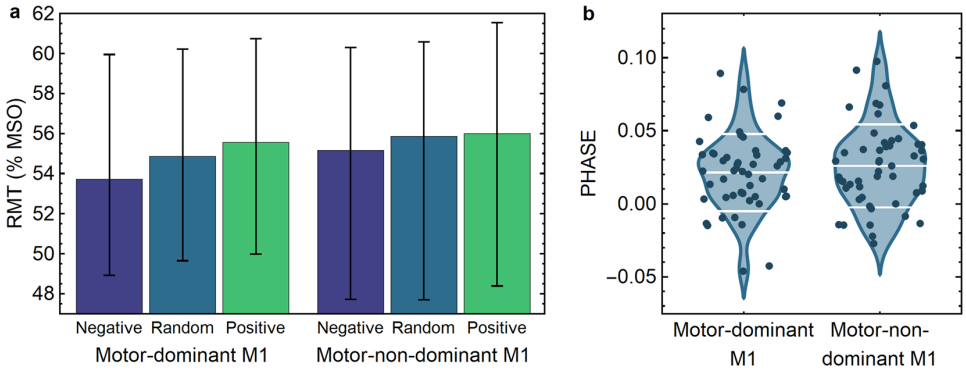

Figure 1. RMT and PHASE for the different stimulation conditions. (**a**) RMT as a percentage of the maximum stimulator output (%MSO). The bars represent the median over subjects and the whiskers indicate the interquartile ranges. (**b**) PHASE = $(RMT_{pos} - RMT_{neg})/RMT_{rand}$ for the motor-dominant and motor-non-dominant hemisphere. The dots show the data of the individual subjects. The white bars indicate the mean and the mean ± standard deviation of the data.

Hemispheric lateralization is a salient organizational feature of the motor system[12]. On the functional level, neuroimaging studies have indicated major differences in movement-associated activation patterns between the motor-dominant and motor-non-dominant hemispheres[13], while TMS studies have shown significant interhemispheric differences between the cortical motor representation areas[14] and the stimulation intensities required to elicit motor responses from the two M1 (with the motor-dominant hemisphere typically requiring lower stimulation intensities than the motor-non-dominant hemisphere)[15,16]. On the structural level, alongside interhemispheric differences in transcallosal[17] and cortico-cortical M1 connectivity[18], significant interhemispheric differences in local intracortical M1 circuits are noted[19]. For example, regional asymmetries of cortical thickness and local gyrification between the hand-knob areas of the two M1 have been associated with the degree of handedness, with evidence of robust leftward asymmetries (i.e., greater gyrification and cortical thickness in the motor-dominant M1) in consistent right-handers[20]. An increased intracortical connectivity within the motor-dominant M1 has also been supported by histological studies, which have shown increased neuropil concentrations (as an indirect measure of intracortical connectivity) within the motor-dominant compared to the motor-non-dominant M1[21].

The motor output neurons in M1 are thought to be activated by TMS mainly transsynaptically through excitation of long-range cortico-cortical axons at the precentral and postcentral gyrus crowns, where the TMS-induced electrical field is strongest[22]. On the other hand, recent studies have shown that the cortical μ-oscillatory activity is regulated – alongside subcortical (i.e., thalamic) inputs – by local feedforward and feedback processes within superficial cortical layers in M1 (e.g., the supragranular pyramidal neurons[23,24]).

In the present study, we were interested in the possible asymmetries of μ-phase-dependency of corticospinal excitability, assessed via brain-state-dependent EEG-triggered TMS-determined resting motor threshold (RMT), between the homologous hand areas of the two M1 in consistently right-handed healthy subjects. To this end, we examined the interhemispheric correlation of the μ-rhythm phase effects (PHASE) on RMT between the two M1, assessing to what extent the μ-oscillation-dependency of corticospinal excitability may be regarded as a ubiquitous physiological trait of the motor system at rest or, alternatively, shows significant hemispheric asymmetry.

Results

All procedures were well tolerated and no adverse events were noted. Based on the predefined inclusion criteria (see Methods), 51 (54%) out of 95 screened subjects were included in this study.

RMT in different pre-stimulus μ-phase conditions. *Motor-dominant primary motor cortex.* RMT differed significantly depending on the pre-stimulus phase of the μ-rhythm, $\chi^2(2)=34.756$, $p < 0.001$ (Fig. 1). Pairwise comparisons were performed with a Bonferroni correction for multiple comparisons (statistical significance was accepted at $p < 0.017$). *Post hoc* analyses showed:

(a) A statistically significant difference between the negative-peak [median RMT_{neg}, interquartile range (IQR): 53.70, (11.15)] and the random-phase condition [median RMT_{rand}, (IQR): 54.85, (10.65)], $p = 0.001$.
(b) A statistically significant difference between the negative-peak and the positive-peak condition [median RMT_{pos}, (IQR): 55.55, (11.05)], $p < 0.001$.
(c) A statistically significant difference between the random-phase and the positive-peak condition, $p = 0.009$.

Motor-non-dominant primary motor cortex. RMT differed significantly depending on the pre-stimulus phase of the μ-rhythm, $\chi^2(2) = 34.402$, $p < 0.001$ (Fig. 1). Pairwise comparisons were performed as above with accepted significance at $p < 0.017$. *Post hoc* analyses showed:

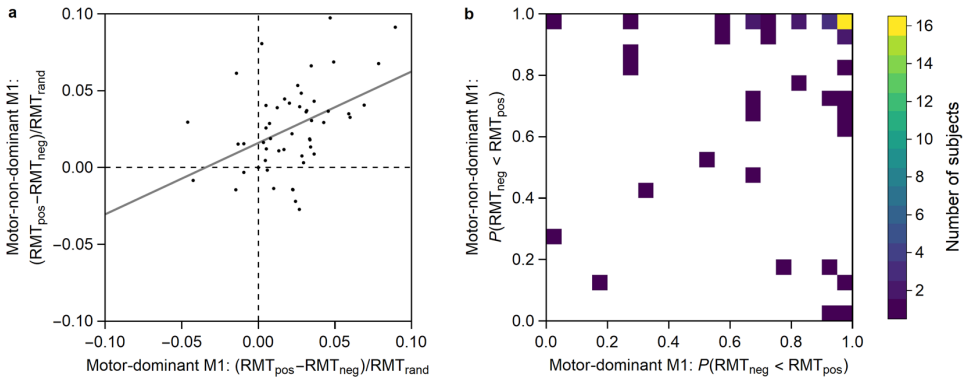

Figure 2. RMT differences for the motor-dominant and motor-non-dominant M1. (**a**) Difference in RMT for each subject between the μ-phase positive-peak and negative-peak conditions. The gray line shows a linear fit to the data. For 40/51 of the subjects (78%), either $RMT_{neg} < RMT_{pos}$ (37/51 subjects, 73%) or $RMT_{pos} < RMT_{neg}$ (3/51 subjects, 6%) was observed in both hemispheres, i.e., their data point is either in the upper right or lower left quadrant of the plot, respectively. **(b)** Number of subjects having a certain probability for $RMT_{neg} < RMT_{pos}$ for the motor-dominant and motor-non-dominant M1. For each subject, the probabilities are obtained from their RMT probability density functions (see Methods, Fig. 3). The number of subjects is reported for adjacent 0.05 × 0.05 squares. The white region marks the area with no subjects.

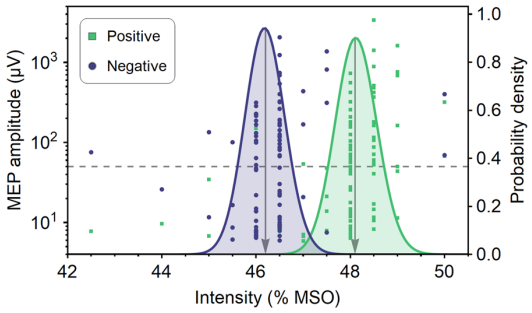

Figure 3. Resting motor threshold. MEP data of a representative single subject for μ-phase positive-peak and negative-peak conditions and the corresponding probability density functions for the RMT. The dashed line indicates the 50 μV MEP amplitude threshold. The arrows indicate the RMT that corresponds to the location of the maximum of the probability density function.

(a) A statistically significant difference between the negative-peak [median RMT_{neg}, (IQR): 55.15, (12.70)] and the random-phase condition [median RMT_{rand}, (IQR): 55.85, (12.95)], $p = 0.003$.
(b) A statistically significant difference between the negative-peak and the positive-peak condition [median RMT_{pos}, (IQR): 56.00, (13.45)], $p < 0.001$.
(c) A statistically significant difference between the random-phase and the positive-peak condition, $p = 0.005$.

No interhemispheric differences in RMT for each pre-stimulus μ-phase condition. Although the median RMT values of the motor-non-dominant hemisphere appeared larger than those of the motor-dominant hemisphere (Fig. 1a), Wilcoxon signed-rank tests did not show statistically significant interhemispheric differences for the positive-peak ($Z = -0.290$, $p = 0.772$), negative-peak ($Z = -0.043$, $p = 0.965$), or random-phase ($Z = -0.037$, $p = 0.970$) conditions.

No interhemispheric differences in PHASE. Two-tailed paired t-test did not show a significant difference between the PHASE in the motor-dominant M1 [mean, (SD): 0.022, (0.025)] and the motor-non-dominant M1 [0.025, (0.029)], $t(50) = -1.124$, $p = 0.267$; Cohen's $d = 0.11$ (Fig. 1b). The corresponding Bayes factor was 0.276, indicating moderate evidence for PHASE being similar across the hemispheres.

Significant positive correlation of PHASE in the motor-dominant M1 and PHASE in the motor-non-dominant M1. A Pearson product-moment correlation indicated a positive correlation

between PHASE in the motor-dominant M1 and PHASE in the motor-non-dominant M1, which was statistically significant ($r = 0.432$, $n = 51$, $p = 0.002$) (Fig. 2a).

Prevalence of PHASE effects in the motor-dominant vs. motor-non-dominant M1. Of the 51 right-handed subjects participating in this study $RMT_{neg} < RMT_{pos}$ was observed

(a) In both the motor-dominant and motor-non-dominant M1 for 37 subjects (73%),
(b) In the motor-dominant M1 for 43 subjects (84%),
(c) In the motor-non-dominant M1 for 41 subjects (80%).

Probability for RMTneg < RMTpos for the motor-dominant and motor-non-dominant M1. The observed differences in the RMT between the μ-phase positive-peak and negative-peak conditions (Fig. 2a) were associated with corresponding probabilities (Fig. 2b). Of the 51 subjects, for 16 subjects (31%) $P(RMT_{neg} < RMT_{pos}) > 0.95$ was observed for both the motor-dominant and motor-non-dominant M1, for 24 subjects (47%) $P(RMT_{neg} < RMT_{pos}) > 0.95$ for the motor-dominant M1, and for 27 subjects (53%) $P(RMT_{neg} < RMT_{pos}) > 0.95$ for the motor-non-dominant M1 (Fig. 2b).

No correlations between interhemispheric differences in RMT, μ-rhythm peak frequency, or signal-to-noise ratio and the interhemispheric difference in PHASE. The rationale of these exploratory analyses was twofold: 1) As stronger brain-state-dependent modulation of corticospinal excitability occurs at weaker stimulation intensities[6], interhemispheric differences in PHASE could be associated with interhemispheric RMT differences (i.e., differences in stimulation intensities). 2) The real-time phase targeting was based on a fixed frequency band of 8–13 Hz and C3/C4-centered Laplacian spatial filters for the extraction of the sensorimotor μ-rhythm. Thus, we were interested in assessing whether interhemispheric dissimilarities of PHASE could be associated with interhemispheric differences in μ-rhythm peak frequencies or μ-rhythm signal-to-noise ratio (SNR).

We did not find any significant correlations between the interhemispheric difference in PHASE and the interhemispheric differences in RMT ($r = 0.019$, $n = 51$, $p = 0.896$), μ-rhythm peak frequencies ($r = -0.172$, $n = 51$, $p = 0.227$), or μ-rhythm SNR ($r = 0.191$, $n = 51$, $p = 0.176$).

Out of the 51 subjects, 10 had dissimilar PHASE (i.e., $P(RMT_{pos} > RMT_{neg}) > 0.5$ for one hemisphere and < 0.5 for the other), whereas 41 had similar PHASE (i.e., $P(RMT_{pos} > RMT_{neg}) > 0.5$ or < 0.5 for both hemispheres). Subjects with dissimilar PHASE and subjects with similar PHASE across hemispheres had comparable interhemispheric differences of RMT [median, (IQR): 5.5, (6.5) vs. 4.4 (5.5), $U = 194$, $p = 0.794$], μ-rhythm peak frequencies [median, (IQR): 0.1, (0.3) vs. 0.2 (0.4), $U = 160$, $p = 0.259$], and μ-rhythm SNR [median, (IQR): 1.9, (1.8) vs. 1.6 (2.7), $U = 195$, $p = 0.812$].

No interhemispheric differences in pre-stimulus signal power for each pre-stimulus μ-phase condition. Wilcoxon signed-rank tests did not show statistically significant interhemispheric differences of the pre-stimulus signal power in the μ-band for the positive-peak ($Z = -0.562$, $p = 0.574$), negative-peak ($Z = -0.131$, $p = 0.896$), or random-phase ($Z = -0.187$, $p = 0.851$) conditions.

Discussion

In this study, we investigated interhemispheric differences in μ-rhythm phase-dependency of corticospinal excitability between the hand-representation areas of the two M1 in 51 consistently right-handed human subjects, using real-time EEG-triggered TMS. We found no interhemispheric asymmetries in the directionality or effect size of μ-phase-dependency of corticospinal excitability. In particular, our results show a significant positive correlation between the μ-phase-dependency of corticospinal excitability of the motor-dominant and motor-non-dominant M1, and no differences in the extent of this effect between the two hemispheres. In accord with previous studies[2–6], we corroborated that the negative peak of the μ-oscillation corresponds to a high-excitability state of the motor cortices, as reflected by the lower RMT values in the negative-peak condition compared to the positive-peak condition. These findings add to the previous results, as RMT was used here for the first time as a readout of corticospinal excitability, whilst in all previous studies the effect of pre-stimulus phase of μ-oscillations on corticospinal excitability had been assessed by large-amplitude MEPs[2–6]. This is an important methodological difference, as small MEPs around RMT are generated by different mechanisms than large MEPs, which are elicited by clearly suprathreshold stimulation intensities. Small MEPs originate predominantly from local monosynaptic activation (i.e., they are reflected in I1-waves), whereas large MEPs are produced by polysynaptic activation through long-range cortico-cortical and subcortical–cortical projections (i.e., they are reflected in late I-waves)[25,26]. Therefore, the observed changes in RMT reflect more closely the μ-phase effects on the excitability of the corticospinal neuron *per se*, as opposed to the previously observed changes in large MEP amplitudes, which may reflect alterations in an extended sensorimotor network.

In the present study, we also systematically investigated the prevalence of μ-phase-dependency of corticospinal excitability in the so-far largest cohort of consecutively included healthy right-handers, and found that 73% of the included subjects (based on the pre-defined exclusion criteria described in Methods) presented phase-dependency in the form of $RMT_{neg} < RMT_{pos}$ in both hemispheres, while 84% and 80% of the subjects presented this phase-dependency in the motor-dominant and motor-non-dominant hemisphere, respectively. These high prevalences are compatible with our previous observation that the μ-phase effect is most strongly expressed in MEPs of small amplitude[2–6].

With regard to the motor cortices, it is known that, between hemispheres, significant macroanatomical[20,27] and microanatomical[21] side differences exist, with a considerable degree of inter-individual variability[28]. Interhemispheric differences in neuronal circuitry have been developmentally related to functional lateralization[29], and in particular to the direction and degree of handedness[30]. Morphologically, the pyramidal tract presents significant leftward asymmetries in right-handers, with larger volume of descending cortical motor fibers on the left side, at cortical[28] and subcortical level[31]. Hence, it is an implicit assumption that interhemispheric differences in corticospinal excitability, as suggested by electrophysiological studies[15], majorly rely on structural–functional differences in homologous motor pathways. In accord with previous electrophysiological studies[16], our results indicated that RMT values of the motor-non-dominant hemisphere were on average larger than those of the motor-dominant hemisphere; however, these differences did not reach statistical significance, possibly due to methodological aspects, such as the use of a biphasic rather than monophasic current waveform[32]. Given these structural–functional leftward asymmetries in right-handers, we addressed whether stronger μ-phase-dependency of corticospinal excitability could occur when stimulating the motor-dominant compared to the motor-non-dominant M1. However, our results do not support this hypothesis, as no interhemispheric asymmetries in the μ-phase-dependency of corticospinal excitability were noted. These findings, in conjunction with the evidence of a significant positive correlation between the μ-phase-dependency of cortical excitability between the two primary motor cortices, support the proposition that μ-phase-dependency of cortical excitability is an inherent, ubiquitous trait of the motor system at rest.

We acknowledge possible limitations of the present study. First, the order of the tested hemispheres was not randomized, which might have rendered the conditions of two hemispheres dissimilar. Nonetheless, after single-pulse TMS and a delay between the testing of the two M1 in the range of several minutes, no sustained TMS-induced modulation of brain activity in the contralateral hemisphere would be expected[33]. Second, the real-time phase targeting was based on a fixed frequency band of 8–13 Hz and C3/C4-centered Laplacian spatial filters for the extraction of the sensorimotor μ-rhythm. Although the use of individualized frequency bands and spatial filters might have improved our results[5], we showed that the dissimilarities of μ-phase effect (noted in 10 out of 51 subjects between the two M1) were not associated with interhemispheric differences in μ-rhythm peak frequencies or SNR. Third, due to the predefined inclusion criteria of this study (i.e., including only right-handers with prominent sensorimotor μ-rhythm, and excluding subjects with a high motor threshold), further research is warranted to assess the generalizability of the present results.

In conclusion, we found no interhemispheric asymmetries in the directionality or effect size of μ-phase-dependency of corticospinal excitability between the two primary motor cortices. A high prevalence of μ-phase-dependency of cortical excitability was noted, with 73% of the 51 tested subjects having higher RMT in the pre-stimulus μ-positive-peak condition as opposed to the μ-negative-peak condition in both M1. Our findings suggest that μ-phase-dependency of cortical excitability is an inherent, symmetrical trait of the motor system at rest.

Methods

Participants. The study was approved by the local ethics committee of the medical faculty of the University of Tübingen (protocol 716/2014BO2). The experiments were performed in accordance with the Declaration of Helsinki and current TMS safety guidelines[34]. Written informed consent was obtained from all participants prior to their participation. Ninety-five healthy volunteers without a history of neurological or psychiatric disease or use of central nervous system active drugs, alcohol or nicotine were screened to identify 51 (54% of the screened) subjects (29 female and 22 male; mean age ±1 SD: 24 ± 6 years, age range: 18–61 years; all right-handed according to the Edinburgh handedness inventory[35], mean ±1 SD laterality score: 74 ± 26; range: 27–100) that fulfilled the following inclusion criteria: (i) TMS-evoked movement of the left first dorsal interosseous (FDI) muscle at ≤80% of the maximum stimulator output (MSO) intensity; (ii) SNR of the μ-band (8–13 Hz) EEG signal ≥5 dB on the left and right sensorimotor cortices, respectively (with the subject at rest and eyes open; see below for more details)[36]. This criterion ensured that the μ-rhythm was strong enough to enable our algorithm to estimate the instantaneous phase of the EEG signal with sufficient accuracy[2,37]. Twenty-six of the invited 95 subjects failed on the FDI-movement criterion, and 18 on the SNR criterion.

Experimental set-up. We recorded EEG with a TMS-compatible Ag/AgCl sintered ring electrode cap (EasyCap GmbH, Germany) with electrodes at the locations C3, C4, FC1, FC2, FC5, FC6, CP1, CP2, CP5, and CP6 of the 10–20 International system[38]. The reference and ground electrodes were at the locations FCz and POz, respectively. The EEG data were sampled with a 24-bit biosignal amplifier (low-pass filtering at 1250 Hz, DC mode, 5-kHz sampling rate; NeurOne Tesla, Bittium Biosignals Ltd., Finland). EMG was recorded from the left and right FDI with adhesive hydrogel electrodes (Kendall, Covidien, Ireland) in a belly–tendon montage connected to the amplifier recording also the EEG (0.16–1250-Hz bandpass filter, 5-kHz sampling rate).

TMS was administered with a figure-of-eight coil (70-mm winding diameter; PMD70-pCool, MAG & More GmbH, Germany) driven by a PowerMAG stimulator (PowerMAG Research 100 ppTMS, MAG & More GmbH). The applied pulse waveforms were biphasic (160-μs period) with the second, biologically predominantly effective phase of the induced electric field in the cortex being in the lateral–posterior to medial–anterior direction. The stimulation intensity was set through a serial-port connection[39]. The coil position was monitored throughout the experimental session with a neuronavigation system (Localite TMS Navigator, Localite GmbH, Germany) and adjusted if necessary. The subject's head was registered to a standard Montreal Neurological Institute head magnetic resonance image. A vacuum pillow (Vacuform 2.0 surgical cushion, B.u.W. Schmidt GmbH, Germany) and a fixation arm (Super Flex Arm (long), Tonica Elektronik A/S, Denmark) were used to immobilize the head and to maintain a fixed coil placement.

EEG data were preprocessed in real time with a Simulink Real-Time model (R2016a, The MathWorks, Inc., MA, USA) running on a dedicated xPC Target computer with the Simulink Real-Time operating system[2]. The model analyzed the ongoing EEG signals provided by the analog output terminal of the amplifier (amplified, 5-kHz sampling rate, 1250-Hz low-pass filter). The EEG activity corresponding to the left (motor-dominant) and right (motor-non-dominant) M1 was extracted from a Laplacian montage centered at channel C3 (channel C3 minus the mean of the surrounding channels FC1, FC5, CP1, and CP5) and at channel C4 (channel C4 minus the mean of the surrounding channels FC2, FC6, CP2, and CP6), respectively[37]. Another parallel Simulink Real-Time model running on the xPC Target computer controlled the triggering of the TMS device based on the EEG data of the Laplacian montages. First, 500-ms-long sliding windows of the data were forward and backward filtered with a finite impulse response filter (8–13-Hz bandpass). Then, the coefficients for an autoregressive Yule–Walker model (order 30) using 372 ms of the filtered data in the middle of the sliding window were calculated. With the autoregressive model, a 128-ms-long prediction of the signal, centered at the end of the original sliding window, was generated. From this prediction, the instantaneous phase of the signal was estimated by computing an analytic signal with the Hilbert transformation. The TMS device was triggered when a targeted μ-rhythm phase was met, provided that the signal power in the 8–13-Hz band exceed a predetermined threshold. Further details of the real-time system are provided in previous publications[2–6].

Experimental sessions. The experiment started with a 10-min recording of resting-state EEG (eyes open, subject instructed to relax and fixate to a cross at eye level in front of them). If the analysis of the resting-state-EEG data indicated a sufficient signal power in the μ-frequency band in both hemispheres, we proceeded with single-pulse TMS. During TMS, subjects were instructed to keep their hands relaxed and their eyes open and to fixate to a cross in front of them. First, we identified the right-FDI hotspot in the left (motor-dominant) M1 as the coil position and orientation resulting, at a slightly suprathreshold stimulation intensity, in maximal MEP amplitudes[25]. Then, we placed the coil at the hotspot and, with a threshold-tracking technique[40], determined RMT, i.e., the minimum stimulation intensity that would evoke MEPs exceeding 50 μV in peak-to-peak amplitude in 50% of the trials for the right FDI in three conditions: positive peak, negative peak, or random phase of the μ-oscillation in the C3 Laplacian. The threshold tracking was conducted independently for each condition. A Matlab (The MathWorks, Inc.) program detected the peak-to-peak MEP amplitude and adjusted the next stimulation intensity for the corresponding condition according to the threshold-tracking algorithm to match the current RMT estimate. In each of the three μ-phase conditions, we administered 100 stimuli at the intensities suggested by the threshold-tracking algorithm. In accord with previous work[3,6], the administration of 100 stimuli per μ-phase condition was chosen to ensure an adequate number of trials (i.e., after trial removal during the EEG and EMG preprocessing stages) to achieve sufficient statistical power for differentiating phase-specific stimulation effects. The stimulation order was pseudorandomized so that blocks of three consecutive stimuli contained one stimulus targeting each μ-phase condition. The minimum interstimulus interval was 2 s. Finally, we conducted an otherwise identical single-pulse TMS experiment on the right M1 with EMG recording from the left FDI and with stimulus conditions based on the real-time-analyzed EEG signal from the C4 Laplacian.

In contrast to our previous studies[2–6], we tested here RMT rather than MEP amplitude as a marker of corticospinal excitability. The rationale is twofold: (1) We have shown previously that the μ-phase effect on corticospinal excitability is predominantly expressed in small-amplitude MEPs, i.e., close to motor threshold;[2–6] (2) Small MEPs are generated by different mechanisms than large MEPs. The small MEPs originate predominantly from local monosynaptic activation (i.e., they are reflected in I1-waves), whereas large MEPs are produced by polysynaptic activation through long-range cortico-cortical and subcortical–cortical projections (i.e., they are reflected in late I-waves)[25,26]. Therefore, changes in RMT will reflect more closely the μ-phase effects on excitability of the corticospinal neuron *per se*, compared to changes of large MEP amplitudes that would reflect alterations in an extended sensorimotor network.

Data preprocessing. EEG and EMG data were analyzed offline with custom-made Matlab (R2016a or newer) scripts. We calculated the power spectrum of the resting-state EEG data from the C3- and C4-Laplacian signals, respectively, and estimated the SNR of the μ-frequency band signal as the peak of the power spectrum in the 8–13-Hz band after subtracting the 1/f component[5]. The peak frequency was saved for further analysis. The EEG data of the left M1 and right M1 TMS sessions of each subject were analyzed as follows: (1) The C3/C4-Laplacian signals were epoched with respect to the TMS pulses and the average of the signal in a 600-ms-long baseline window immediately preceding the TMS pulse was subtracted from them. (2) The baseline signals of each subject were plotted on top of each other and an individual threshold was visually identified (due to the variable signal characteristics across subjects, the threshold was based on the judgement of the person conducting the analysis) for each subject (separately for the C3/C4-Laplacian signals). (3) Trials with a baseline exceeding the individual threshold were discarded from the subsequent analysis to exclude trials in which noise/artifacts might have compromised the phase estimation.

The EMG data were high-pass filtered at 5 Hz by applying a second-order Butterworth filter in the forward and backward direction, respectively. The EMG data were then epoched with respect to the TMS pulses and baseline-corrected, with the baseline window ranging from −200 to 0 ms with respect to the TMS pulse. The TMS artifact was removed by linearly interpolating the signal between 0 and 10 ms, and the signal was filtered with a second-order Butterworth notch filter (49–51 Hz; applied in both directions) to reduce power-line noise. A fifth-order polynomial was fitted to and subtracted from the baseline data to reduce the effect of a TMS-pulse-related signal drift on the baseline data. The data were then baseline corrected for the second time. Trials containing muscle activation, artifacts, or noise exceeding an individual threshold in a 200-ms period preceding the TMS pulse were discarded, since pre-innervation increases the MEP amplitude[41]. These individual EMG

thresholds for the left and right FDI, respectively, were determined visually by plotting the baseline EMG traces on top of each other (due to the variable signal characteristics across subjects, the thresholds were based on the judgement of the person conducting the analysis). In total, 17% of the trials were discarded. Only 1% of the trials were discarded based on the EEG criteria, and the remaining trials were discarded due to insufficient EMG quality.

Data analysis. The data passing the EEG and EMG preprocessing stages were used for subsequent analysis. For each accepted trial, we determined the MEP peak-to-peak amplitude in a time window of 15–45 ms with respect to the TMS pulse. For each phase condition and subject, we fitted cumulative Gaussians to the MEP data corresponding to the left M1 and right M1 stimulation, respectively[40]. These cumulative Gaussians modeled the probability of obtaining an MEP exceeding 50 μV in peak-to-peak amplitude and allowed us to obtain the probability density for RMT as a function of stimulation intensity (Fig. 3)[40]. The RMT of the right and left FDI, serving as a measure of the corticospinal excitability of the left M1 and right M1, respectively, was identified as the location of the maximum of the corresponding probability density function. We also determined for each subject and hemisphere the probability that the RMT in the positive-peak phase condition was higher than the RMT in the negative-peak phase condition (i.e., $P(RMT_{pos} > RMT_{neg})$) based on the probability density functions. This was achieved by integrating the joint probability density function (defined for stimulation intensities 0–100% MSO) over the triangular area in which the stimulation intensity for the positive-peak phase condition exceeded the intensity for the negative-peak phase condition.

To assess whether the pre-stimulus signal power in the μ-band was similar across hemispheres in all three conditions of phase-dependent RMT estimation, we calculated the average pre-stimulus power for each subject adhering to a previously published pipeline[42]. The following steps were performed: 1) For each accepted trial, we extracted 2 seconds of the C3/C4-Laplacian EEG data centered around the time of the TMS pulse (time 0 ms). 2) We removed the TMS artefact by linearly interpolating the signal from 0 to 15 ms. 3) After applying a second-order Butterworth anti-aliasing filter (cut-off frequency 200 Hz) in forward and backward directions, we downsampled the data to 500 Hz. 4) We estimated the power spectral density with the Burg's method (model order 26; 1-Hz frequency resolution; frequency range: 1–45 Hz) in the time window ranging from −150 to 0 ms with respect to the TMS pulse. 5) After subtracting the 1/f component[5], we extracted the total μ-band power at 8–13 Hz.

Statistical analysis. Statistical analyses were performed with IBM SPSS Statistics v.23 (IBM, NY, USA) and Matlab (The MathWorks, Inc.). The distribution of data was checked with the Shapiro–Wilk test; normally and non-normally distributed data were analyzed with parametric and non-parametric tests, respectively. Differences in the RMT for the different pre-stimulus μ-phase conditions, i.e., the negative (neg) and positive (pos) peaks of a Laplacian signal and the random phase (rand), were assessed using Friedman tests (due to non-normal distributions). Wilcoxon signed-rank tests were used to assess the interhemispheric differences in RMT for each condition. Also, Wilcoxon signed-rank tests were used to assess possible interhemispheric differences in the average pre-stimulus signal power for each condition. We defined PHASE as $(RMT_{pos} - RMT_{neg})/RMT_{rand}$. To assess whether PHASE in the left M1 was correlated with PHASE in the right M1, Pearson's correlation analysis was performed (after confirming linear relationship between the variables, and normal distribution of the data). A two-tailed paired t-test was used to assess differences in PHASE between hemispheres (in addition to the *p* value, we calculated also the corresponding Bayes factor with the bayesFactor Matlab toolbox[43]). The prevalence of PHASE and probabilities for $RMT_{neg} < RMT_{pos}$ in each hemisphere were also calculated. To assess whether interhemispheric differences of PHASE were correlated with interhemispheric differences of RMT (i.e., RMT_{rand}), μ-rhythm peak frequencies, or SNR, Pearson's correlation analyses were performed. In an exploratory analysis, interhemispheric differences in RMT, μ-rhythm peak frequencies, and SNR were assessed in subjects with $P(RMT_{pos} > RMT_{neg}) > 0.5$ for one hemisphere and <0.5 for the other (i.e., dissimilar PHASE across hemispheres) vs. subjects with $P(RMT_{pos} > RMT_{neg}) > 0.5$ or <0.5 for both hemispheres (i.e., similar PHASE across hemispheres) using Mann-Whitney U tests (due to non-normal distributions). The significance level was set for all statistical tests to <0.05 (unless stated otherwise).

Data availability

Data are available from the corresponding author upon reasonable request.

Received: 25 January 2020; Accepted: 15 April 2020;
Published online: 12 May 2020

References

1. Haegens, S., Nácher, V., Luna, R., Romo, R. & Jensen, O. α-oscillations in the monkey sensorimotor network influence discrimination performance by rhythmical inhibition of neuronal spiking. *Proc Natl Acad Sci U S A* **108**, 19377–19382, https://doi.org/10.1073/pnas.1117190108 (2011).
2. Zrenner, C., Desideri, D., Belardinelli, P. & Ziemann, U. Real-time EEG-defined excitability states determine efficacy of TMS-induced plasticity in human motor cortex. *Brain Stimul* **11**, 374–389, https://doi.org/10.1016/j.brs.2017.11.016 (2018).
3. Stefanou, M. I. *et al.* Brain state-dependent brain stimulation with real-time electroencephalography-triggered transcranial magnetic stimulation. *J Vis Exp* https://doi.org/10.3791/59711 (2019).
4. Stefanou, M. I., Desideri, D., Belardinelli, P., Zrenner, C. & Ziemann, U. Phase synchronicity of μ-rhythm determines efficacy of interhemispheric communication between human motor cortices. *J Neurosci* **38**, 10525–10534, https://doi.org/10.1523/JNEUROSCI.1470-18.2018 (2018).
5. Schaworonkow, N. *et al.* rhythm extracted with personalized EEG filters correlates with corticospinal excitability in real-time phase-triggered EEG-TMS. *Front Neurosci* **12**, 954, https://doi.org/10.3389/fnins.2018.00954 (2018).
6. Schaworonkow, N., Triesch, J., Ziemann, U., Zrenner, C. & EEG-triggered, T. M. S. reveals stronger brain state-dependent modulation of motor evoked potentials at weaker stimulation intensities. *Brain Stimul* **12**, 110–118, https://doi.org/10.1016/j.brs.2018.09.009 (2019).

7. Hari, R. Action–perception connection and the cortical mu rhythm. *Prog Brain Res* **159**, 253–260, https://doi.org/10.1016/S0079-6123(06)59017-X (2006).
8. Mathewson, K. E. *et al*. Pulsed out of awareness: EEG alpha oscillations represent a pulsed-inhibition of ongoing cortical processing. *Front Psychol* **2**, 99, https://doi.org/10.3389/fpsyg.2011.00099 (2011).
9. Storm van Leeuwen, W., Arntz, A., Spoelstra, P. & Wieneke, G. H. The use of computer analysis for diagnosis in routine electroencephalography. *Rev Electroencephalogr Neurophysiol Clin* **6**, 318–327, https://doi.org/10.1016/s0370-4475(76)80111-6 (1976).
10. Pineda, J. A. The functional significance of mu rhythms: translating "seeing" and "hearing" into "doing". *Brain Res Rev* **50**, 57–68, https://doi.org/10.1016/j.brainresrev.2005.04.005 (2005).
11. Amunts, K., Jäncke, L., Mohlberg, H., Steinmetz, H. & Zilles, K. Interhemispheric asymmetry of the human motor cortex related to handedness and gender. *Neuropsychologia* **38**, 304–312, https://doi.org/10.1016/s0028-3932(99)00075-5 (2000).
12. Güntürkün, O. & Ocklenburg, S. Ontogenesis of lateralization. *Neuron* **94**, 249–263, https://doi.org/10.1016/j.neuron.2017.02.045 (2017).
13. Sainburg, R. L. Evidence for a dynamic-dominance hypothesis of handedness. *Exp Brain Res* **142**, 241–258, https://doi.org/10.1007/s00221-001-0913-8 (2002).
14. Triggs, W. J., Subramanium, B. & Rossi, F. Hand preference and transcranial magnetic stimulation asymmetry of cortical motor representation. *Brain Res* **835**, 324–329, https://doi.org/10.1016/s0006-8993(99)01629-7 (1999).
15. Ilic, T. V., Jung, P. & Ziemann, U. Subtle hemispheric asymmetry of motor cortical inhibitory tone. *Clin Neurophysiol* **115**, 330–340, https://doi.org/10.1016/j.clinph.2003.09.017 (2004).
16. Netz, J., Ziemann, U. & Hömberg, V. Hemispheric asymmetry of transcallosal inhibition in man. *Exp Brain Res* **104**, 527–533, https://doi.org/10.1007/bf00231987 (1995).
17. Karolis, V. R., Corbetta, M. & de Schotten, M. T. The architecture of functional lateralisation and its relationship to callosal connectivity in the human brain. *Nat Commun* **10**, 1417, https://doi.org/10.1038/s41467-019-09344-1 (2019).
18. Schlerf, J. E., Galea, J. M., Spampinato, D. & Celnik, P. A. Laterality differences in cerebellar–motor cortex connectivity. *Cereb Cortex* **25**, 1827–1834, https://doi.org/10.1093/cercor/bht422 (2015).
19. Cicinelli, P. *et al*. Intracortical excitatory and inhibitory phenomena to paired transcranial magnetic stimulation in healthy human subjects: differences between the right and left hemisphere. *Neurosci Lett* **288**, 171–174, https://doi.org/10.1016/s0304-3940(00)01216-7 (2000).
20. McDowell, A., Felton, A., Vazquez, D. & Chiarello, C. Neurostructural correlates of consistent and weak handedness. *Laterality* **21**, 348–370, https://doi.org/10.1080/1357650X.2015.1096939 (2016).
21. Amunts, K. *et al*. Asymmetry in the human motor cortex and handedness. *Neuroimage* **4**, 216–222, https://doi.org/10.1006/nimg.1996.0073 (1996).
22. Laakso, I., Murakami, T., Hirata, A. & Ugawa, Y. Where and what TMS activates: Experiments and modeling. *Brain Stimul* **11**, 166–174, https://doi.org/10.1016/j.brs.2017.09.011 (2018).
23. Jones, S. R. *et al*. Quantitative analysis and biophysically realistic neural modeling of the MEG mu rhythm: rhythmogenesis and modulation of sensory-evoked responses. *J Neurophysiol* **102**, 3554–3572, https://doi.org/10.1152/jn.00535.2009 (2009).
24. Haegens, S. *et al*. Laminar profile and physiology of the α rhythm in primary visual, auditory, and somatosensory regions of neocortex. *J Neurosci* **35**, 14341–14352, https://doi.org/10.1523/JNEUROSCI.0600-15.2015 (2015).
25. Rossini, P. M. *et al*. Non-invasive electrical and magnetic stimulation of the brain, spinal cord, roots and peripheral nerves: Basic principles and procedures for routine clinical and research application. An updated report from an I.F.C.N. Committee. *Clin Neurophysiol* **126**, 1071–1107, https://doi.org/10.1016/j.clinph.2015.02.001 (2015).
26. Di Lazzaro, V., Ziemann, U. & Lemon, R. N. State of the art: Physiology of transcranial motor cortex stimulation. *Brain Stimul* **1**, 345–362, https://doi.org/10.1016/j.brs.2008.07.004 (2008).
27. Thompson, P. M., Schwartz, C., Lin, R. T., Khan, A. A. & Toga, A. W. Three-dimensional statistical analysis of sulcal variability in the human brain. *J Neurosci* **16**, 4261–4274, https://doi.org/10.1523/JNEUROSCI.16-13-04261.1996 (1996).
28. Rademacher, J. *et al*. Variability and asymmetry in the human precentral motor system. A cytoarchitectonic and myeloarchitectonic brain mapping study. *Brain* **124**, 2232–2258, https://doi.org/10.1093/brain/124.11.2232 (2001).
29. Geschwind, N. & Galaburda, A. M. Cerebral lateralization. Biological mechanisms, associations, and pathology: III. A hypothesis and a program for research. *Arch Neurol* **42**, 634–654, https://doi.org/10.1001/archneur.1985.04060070024012 (1985).
30. Volkmann, J., Schnitzler, A., Witte, O. W. & Freund, H. Handedness and asymmetry of hand representation in human motor cortex. *J Neurophysiol* **79**, 2149–2154, https://doi.org/10.1152/jn.1998.79.4.2149 (1998).
31. Virta, A., Barnett, A. & Pierpaoli, C. Visualizing and characterizing white matter fiber structure and architecture in the human pyramidal tract using diffusion tensor MRI. *Magn Reson Imaging* **17**, 1121–1133, https://doi.org/10.1016/s0730-725x(99)00048-x (1999).
32. Sommer, M. *et al*. TMS of primary motor cortex with a biphasic pulse activates two independent sets of excitable neurones. *Brain Stimul* **11**, 558–565, https://doi.org/10.1016/j.brs.2018.01.001 (2018).
33. Mutanen, T., Nieminen, J. O. & Ilmoniemi, R. J. TMS-evoked changes in brain-state dynamics quantified by using EEG data. *Front Hum Neurosci* **7**, 155, https://doi.org/10.3389/fnhum.2013.00155 (2013).
34. Rossi, S., Hallett, M., Rossini, P. M. & Pascual-Leone, A. The Safety of TMS Consensus Group. Safety, ethical considerations, and application guidelines for the use of transcranial magnetic stimulation in clinical practice and research. *Clin Neurophysiol* **120**, 2008–2039, https://doi.org/10.1016/j.clinph.2009.08.016 (2009).
35. Oldfield, R. C. The assessment and analysis of handedness: the Edinburgh inventory. *Neuropsychologia* **9**, 97–113, https://doi.org/10.1016/0028-3932(71)90067-4 (1971).
36. Nikulin, V. V. & Brismar, T. Phase synchronization between alpha and beta oscillations in the human electroencephalogram. *Neuroscience* **137**, 647–657, https://doi.org/10.1016/j.neuroscience.2005.10.031 (2006).
37. Hjorth, B. An on-line transformation of EEG scalp potentials into orthogonal source derivations. *Electroencephalogr Clin Neurophysiol* **39**, 526–530, https://doi.org/10.1016/0013-4694(75)90056-5 (1975).
38. Seeck, M. *et al*. The standardized EEG electrode array of the IFCN. *Clin Neurophysiol* **128**, 2070–2077, https://doi.org/10.1016/j.clinph.2017.06.254 (2017).
39. Habibollahi Saatlou, F. *et al*. MAGIC: An open-source MATLAB toolbox for external control of transcranial magnetic stimulation devices. *Brain Stimul* **11**, 1189–1191, https://doi.org/10.1016/j.brs.2018.05.015 (2018).
40. Awiszus, F. TMS and threshold hunting. *Suppl Clin Neurophysiol* **56**, 13–23 (2003).
41. Hallett, M. Transcranial magnetic stimulation: a primer. *Neuron* **55**, 187–199, https://doi.org/10.1016/j.neuron.2007.06.026 (2007).
42. Hussain, S. J. *et al*. Sensorimotor Oscillatory Phase-Power Interaction Gates Resting Human Corticospinal Output. *Cereb Cortex* **29**, 3766–3777, https://doi.org/10.1093/cercor/bhy255 (2019).
43. Krekelberg, B. *bayesFactor*. *GitHub*, https://www.github.com/klabhub/bayesFactor, (2019).

Acknowledgements
The authors thank Nicole Knodel and David Baur for their help in the experiments. The project has received funding from the Academy of Finland (Decisions No. 294625 and 306845) and from the European Research Council (ERC) under the European Union's Horizon 2020 research and innovation programme (grant agreement No 810377).

Author contributions
M.-I.S., D.G., C.Z., U.Z. and J.O.N. designed the experiment and data-analysis methods. M.-I.S., D.G. and J.O.N. performed the experiments. M.-I.S. and J.O.N. analyzed the data. M.-I.S. and J.O.N. wrote the article. U.Z. revised the manuscript. All the authors reviewed the manuscript.

Competing interests
The authors declare no competing interests.

Additional information
Correspondence and requests for materials should be addressed to U.Z.

Reprints and permissions information is available at www.nature.com/reprints.

Publisher's note Springer Nature remains neutral with regard to jurisdictional claims in published maps and institutional affiliations.

Systems/Circuits

Phase Synchronicity of μ-Rhythm Determines Efficacy of Interhemispheric Communication Between Human Motor Cortices

Maria-Ioanna Stefanou,* Debora Desideri,* Paolo Belardinelli, Christoph Zrenner, and Ulf Ziemann
Department of Neurology and Stroke and Hertie Institute for Clinical Brain Research, Eberhard-Karls University of Tübingen, 72076 Tübingen, Germany

The theory of communication through coherence predicts that effective connectivity between nodes in a distributed oscillating neuronal network depends on their instantaneous excitability state and phase synchronicity (Fries, 2005). Here, we tested this prediction by using state-dependent millisecond-resolved real-time electroencephalography-triggered dual-coil transcranial magnetic stimulation (EEG-TMS) (Zrenner et al., 2018) to target the EEG-negative (high-excitability state) versus EEG-positive peak (low-excitability state) of the sensorimotor μ-rhythm in the left (conditioning) and right (test) motor cortex (M1) of 16 healthy human subjects (9 female, 7 male). Effective connectivity was tested by short-interval interhemispheric inhibition (SIHI); that is, the inhibitory effect of the conditioning TMS pulse given 10–12 ms before the test pulse on the test motor-evoked potential. We compared the four possible combinations of excitability states (negative peak, positive peak) and phase relations (in-phase, out-of-phase) of the μ-rhythm in the conditioning and test M1 and a random phase condition. Strongest SIHI was found when the two M1 were in phase for the high-excitability state (negative peak of the μ-rhythm), whereas the weakest SIHI occurred when they were out of phase and the conditioning M1 was in the low-excitability state (positive peak). Phase synchronicity contributed significantly to SIHI variation, with stronger SIHI in the in-phase than out-of-phase conditions. These findings are in exact accord with the predictions of the theory of communication through coherence. They open a translational route for highly effective modification of brain connections by repetitive stimulation at instants in time when nodes in the network are phase synchronized and excitable.

Key words: communication through coherence; EEG-TMS; effective cortico-cortical connectivity; human; interhemispheric communication; motor cortex

Significance Statement

The theory of communication through coherence predicts that effective connectivity between nodes in distributed oscillating brain networks depends on their instantaneous excitability and phase relation. We tested this hypothesis in healthy human subjects by real-time analysis of brain states by electroencephalography in combination with transcranial magnetic stimulation of left and right motor cortex. We found that short-interval interhemispheric inhibition, a marker of interhemispheric effective connectivity, was maximally expressed when the two motor cortices were in phase for a high-excitability state (the trough of the sensorimotor μ-rhythm). We conclude that findings are consistent with the theory of communication through coherence. They open a translational route to highly effectively modify brain connections by repetitive stimulation at instants in time of phase-synchronized high-excitability states.

Introduction

Neuronal assemblies in the brain oscillate and thereby undergo rhythmic fluctuations of excitation and inhibition (Buzsáki and Draguhn, 2004; Jensen and Mazaheri, 2010). The theory of communication through coherence (CTC) (Fries, 2005, 2015) predicts that coherently oscillating neuronal assemblies in distributed

Received June 10, 2018; revised Oct. 14, 2018; accepted Oct. 15, 2018.

Author contributions: M.-I.S., D.D., P.B., and C.Z. wrote the first draft of the paper; U.Z. edited the paper; U.Z. designed research; M.-I.S., D.D., P.B., and C.Z. performed research; M.-I.S., D.D., P.B., C.Z., and U.Z. analyzed data; U.Z. wrote the paper.

This work was supported by the Deutsche Forschungsgemeinschaft (Grant ZI 542/7-1 to U.Z.), the Federal Ministry of Education and Research (BMBF MOTOR-BIC Grant to U.Z.), and the University of Tübingen (Fortüne Junior Grant 2287-0-0 to C.Z.).

The authors declare no competing financial interests.

*M.-I.S. and D.D. contributed equally to this work.

Correspondence should be addressed to Dr. Ulf Ziemann, Department of Neurology and Stroke and Hertie Institute for Clinical Brain Research, Eberhard-Karls University of Tübingen, Hoppe-Seyler-Str. 3, 72076 Tübingen, Germany. E-mail: ulf.ziemann@uni-tuebingen.de.

https://doi.org/10.1523/JNEUROSCI.1470-18.2018

 0270-6474/18/3810525-10$15.00/0

cortical networks interact effectively in synchronized states of high excitability (Womelsdorf et al., 2007). CTC is considered fundamental for all higher cognitive and sensorimotor brain functions (Singer, 1999; Varela et al., 2001; Uhlhaas and Singer, 2010). Early experimental evidence for CTC in bihemispheric networks came from studies in cats that revealed that interhemispheric oscillatory synchronization between homologous neural assemblies in primary visual cortex is critical for the binding of distributed features of neural information in the two visual hemifields (Engel et al., 1991). In the motor domain, 20–40 Hz oscillations in monkey primary motor cortices (M1) of the two hemispheres transiently synchronize during bimanual and unimanual motor tasks (Murthy and Fetz, 1996) and, in human motor cortex, paired-pulse transcranial magnetic stimulation (TMS) experiments revealed that inhibitory motor signals are transmitted in beta bursts in large-scale motor cortical networks for inhibitory motor control (Picazio et al., 2014).

Here, we sought to test one of the core predictions of the CTC theory that effective communication critically depends on the phase relation between neuronal assemblies, for inhibitory interhemispheric motor activity at the systems level in humans. Interhemispheric effective connectivity can be measured by a dual-coil paired-pulse TMS protocol that results in short-interval interhemispheric inhibition (SIHI) of motor evoked potentials (MEPs) if the two pulses are given to the conditioning and test M1 ~10 ms apart (Ferbert et al., 1992; Daskalakis et al., 2002). For testing phase relations of the ongoing sensorimotor μ-rhythm, we made use of a recently developed technique that allows analysis of μ-rhythm phase with electroencephalography (EEG) in real time and triggering of TMS pulses at prespecified phase (Zrenner et al., 2018).

The μ-rhythm constitutes the dominant rhythm in the frequency spectrum of the sensorimotor cortex at rest (Hari, 2006; Haegens et al., 2011). The negative versus positive peaks of the μ-rhythm in EEG represent states of high versus low excitability of corticospinal neurons as measured by MEP amplitude (Zrenner et al., 2018). Although corticospinal neurons and output neurons projecting to the M1 in the opposite hemisphere form segregate assemblies in different cortical layers (Jones and Wise, 1977), it is likely that their excitability states are linked, as indicated by common variation of conditioning MEP amplitude and SIHI (Ferbert et al., 1992; Ni et al., 2009; Ghosh et al., 2013).

Using the novel EEG-TMS technique (Zrenner et al., 2018), we tested here the effects of four different specific states of the conditioning and test M1 on effective interhemispheric connectivity expressed by SIHI: in phase for the high-excitability state (negative peak of the μ-rhythm) or the low-excitability state (positive peak) or out of phase (conditioning M1 either at negative or positive peak and test M1 at the opposite phase). Consistent with the CTC theory, we hypothesized that the strongest SIHI will occur when the conditioning and test M1 are in phase for the high-excitability state; that is, when the two M1 communicate and input is maximal from the conditioning to test M1. Furthermore, we expected the weakest SIHI when the two M1 are out of phase with the conditioning M1 in the low-excitability state.

We consider this research as of high importance because demonstration of CTC at the systems level of the human brain will open the possibility to highly effectively modify brain connections by repetitive stimulation of the nodes of that connection at instants in time when they are phase synchronized.

Materials and Methods

Subjects. The study protocol was approved by the local ethics committee of the medical faculty of the University of Tübingen (protocol 716/2014BO2). The experiments conformed to the Declaration of Helsinki and were performed in accordance with the current TMS safety guidelines of the International Federation of Clinical Neurophysiology (Rossi et al., 2009). All subjects provided written informed consent before participation. Thirty healthy volunteers without a history of neurological or psychiatric disease or use of CNS active drugs, alcohol, or nicotine were screened. Sixteen subjects (9 female and 7 male; all right-handed according to the Edinburgh handedness inventory; mean age ±1 SD 29.0 ± 9.5 years; age range: 22–53 years) fulfilled all of the following inclusion criteria (Zrenner et al., 2018): (1) resting motor threshold (RMT) of the right and left abductor pollicis brevis (APB) and/or right and left first dorsal interosseous (FDI) muscle ≤70% of maximum stimulator output (MSO); (2) stimulus intensity necessary to evoke MEP of 1 mV in peak-to-peak amplitude ($SI_{1\ mV}$) ≤130% of RMT; (3) single peak in the μ-band (8–12 Hz) >25% of total power in the current source density (CSD) power spectrum of the C3 and C4 EEG signals representing neural activity in the left and right sensorimotor cortices, respectively, with the subject at rest and eyes open; (4) at the stimulation intensities selected according to criteria 1 and 2 SIHI (percentage of conditioned over unconditioned MEP) ≤90%. Threshold criteria 1 and 2 were selected to ensure that the TMS stimulator would be able to perform at the required intensities for the whole duration of the experiment. Criterion 3 ensured that the oscillation amplitudes were adequately large to enable our algorithm to estimate instantaneous phase of the trigger signal with sufficient accuracy (Hjorth, 1975; Zrenner et al., 2018). Twelve of 14 of the excluded subjects failed on the CSD power spectrum criterion and two of 14 subjects on the SIHI criterion.

Experimental setup. The present study was conducted based on a real-time, millisecond-resolution brain-state-dependent EEG-triggered TMS system that has been recently developed in our laboratory (Zrenner et al., 2018). This EEG-TMS setup uses an online output of the raw EEG signal and analyzes it in real time to trigger TMS pulses depending on the instantaneous oscillatory phase of the recorded EEG. For the experiments of the present study, the stimulation setup consisted of two passively cooled TMS double coils (PMD45-pCool, 45 mm winding diameter, MAG & More) and two high-frequency magnetic stimulators (Research 100, MAG & More) to deliver biphasic single cosine cycle pulses with a 160 μs period. The stimulator delivering the test stimulus (TS) was connected to a coil placed optimally over the hand representation area (the "hotspot," see below) of the right M1, with the handle of the coil pointing backward and ~45 degrees to the midsagittal line. The stimulator delivering the conditioning stimulus (CS) was connected to a coil placed similarly over the hand representation area of the left M1, but slight repositioning and reorienting of this coil was necessary in most of the subjects to fit both coils tangentially on the scalp (mean ±1 SD coil angle over left M1 relative to the central sulcus: 30.6°±16.5°). The chosen orientation of the coils ensured that the second phase of the biphasic pulse induced an electrical field in the brain from lateral–posterior to medial–anterior. This current orientation is effective in *trans*-synaptically activating corticospinal neurons and inducing corticocortical, interhemispheric interactions (Ferbert et al., 1992; Daskalakis et al., 2002). For both hemispheres, the motor hotspots were identified as the coil position and orientation resulting at a slightly suprathreshold stimulation intensity in maximum MEP amplitudes (Rossini et al., 2015). A vacuum pillow (Vacuform, B.u.W. Schmidt) and two fixation arms (Magic Arm, Lino Manfrotto) were used to immobilize the head and maintain fixed coil positions over the motor hotspots during the experiment. The magnetic stimulators were triggered through a transistor–transistor logic (TTL) trigger input from the real-time digital signal processing system. Stimulus intensities were set manually.

A stereoscopic neuronavigation system (Localite, RRID:SCR_016126) was used to register the subject's head to a standard Montreal Neurological Institute (MNI) brain anatomical dataset to record the coordinates of the motor hotspots and monitor throughout the experimental session the position of the two TMS coils in 3D space relative to the subject's head

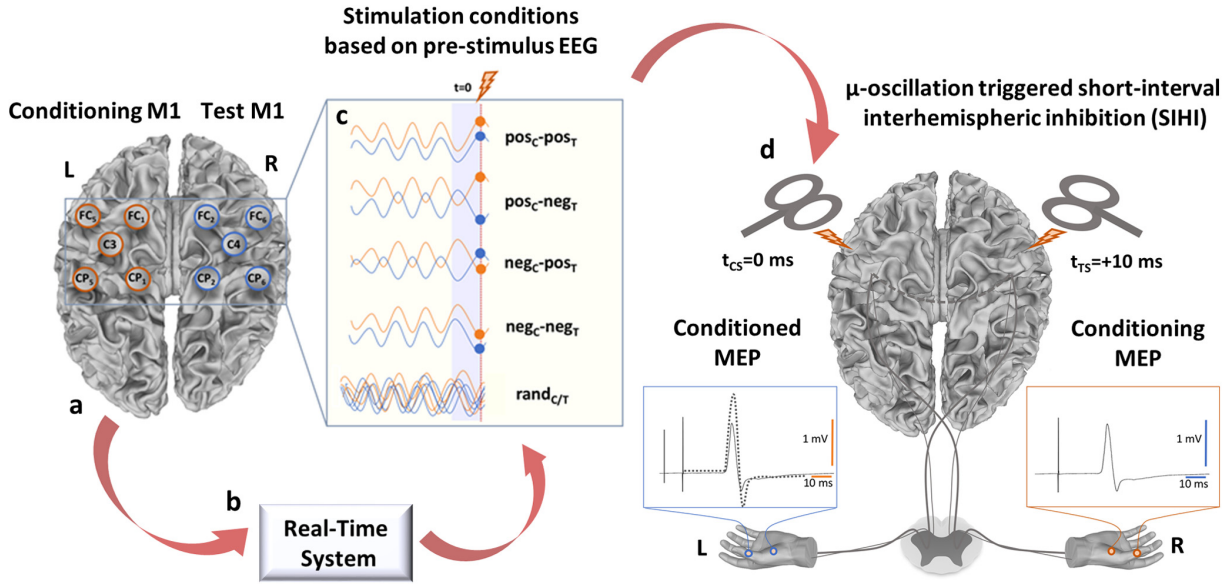

Figure 1. μ-oscillation triggered SIHI. ***a***, ***b***, Scalp EEG raw data derived from 5-point sum-of-difference operators centered on the C3 and C4 EEG electrodes (Hjorth-C3 and Hjorth-C4) over the left and right sensorimotor cortices are streamed to a real-time system with 3 ms latency (***a***), where a processing algorithm is computed at a rate of 500 Hz (***b***). The EEG-data are 8–12 Hz band-pass filtered forward and backward, edge artifacts are removed, and coefficients for an autoregressive model are calculated from the filtered data. ***c***, ***d***, The signal is forward predicted (blue shaded area in ***c***), phase is estimated at time 0 ($t = 0$) using a Hilbert transform, and the two TMS stimulators (***d***) are triggered at 0 ms (CS to the hand area left motor cortex) and +10 ms or (in half of the subjects) +12 ms (test stimulus TS to the hand area right motor cortex) when the preselected one of the five predefined phase conditions (***c***) is met in the Hjorth-C3 (orange) and Hjorth-C4 (blue) EEG signals. These correspond to the four possible combinations of positive (pos) and negative (neg) peaks of the ongoing sensorimotor μ-rhythm in the conditioning (C) and the test (T) M1 (pos$_C$-pos$_T$, pos$_C$-neg$_T$, neg$_C$-pos$_T$, neg$_C$-neg$_T$) and a random phase condition as control (rand$_{C/T}$). ***d***, Short-interval interhemispheric inhibition is reflected by attenuation of the conditioned MEP (continuous line) compared with the nonconditioned test MEP (dotted line) recorded by surface EMG from the left-hand target muscles (only EMG electrodes on APB are shown; electrodes on first dorsal interosseus are not shown).

and to acquire the position of the coils at each TMS pulse. Manual adjustments of coil position were performed in case of coil displacement.

Scalp EEG was recorded from a 64-channel TMS compatible Ag/AgCl sintered ring electrode cap (EasyCap) according to the 10–20 international system (Seeck et al., 2017). A 24-bit 80-channel biosignal amplifier was used for EEG recordings (NeurOne tesla with Analog Out Option, Bittium Biosignals). The data were acquired in DC mode with a headstage sampling rate of 80 kHz for subsequent analysis. The analog output option of the amplifier was configured to recreate from the digital data a filtered and amplified parallel analog signal (5 kHz sampling rate per channel, 1.25 kHz low-pass anti-aliasing filter) from a user-selectable subset of 16 amplifier channels covering left and right sensorimotor cortices. Out of this subset, 5-point "sum-of-difference" operators centered on C3 with surrounding electrodes FC1, FC5, CP1 and CP5 [(C3 − FC1) + (C3 − FC5) + (C3 − CP1) + (C3 − CP5), referred to as Hjorth-C3] and C4 with surrounding electrodes FC2, FC6, CP2 and CP6 [(C4 − FC2) + (C4 − FC6) + (C4 − CP2) + (C4 − CP6), referred to as Hjorth-C4] (Hjorth, 1975) were calculated by the real-time system at a rate of 500 Hz as orthogonal source derivations to isolate local sensorimotor μ-oscillations from signal contamination by volume conduction and interference from other sources of alpha oscillations. The analog output stage consisted of a 16-bit digital-to-analog converter (DAC) system with a 10 kHz frequency and a signal conditioning stage to produce a low-pass-filtered (500 Hz cutoff frequency, 24 dB/octave), scaled signal in the ±5 V range, resolving sensor data at 0.1 μV. The analog-to-digital conversion (ADC), digital filtering, DAC stage, and signal conditioning stage resulted in a constant latency of 3 ms between the signal at the EEG sensor and the signal at the analog output (Fig. 1).

MEPs were recorded by surface EMG using bipolar adhesive hydrogel electrodes (Kendall, Covidien) over the voluntarily relaxed left and right APB and FDI muscles in a belly-tendon montage (5 kHz sampling rate, 0.16 Hz to 1.25 kHz band-pass filter) and using the 24-bit 80-channel biosignal amplifier (NeurOne Tesla with Analog Out Option, Bittium Biosignals).

Real-time digital signal processing. Running in parallel to the wide-bandwidth 24-bit resolution 5 kHz recording and archiving of the raw EEG data, a real-time data acquisition, digital processing, and magnetic stimulator control system was implemented as a Simulink Real-Time model (The MathWorks, R2016a, RRID:SCR_014744) executed on a dedicated xPC Target PC running the Simulink Real-Time operating system (DFI-ACP CL630-CRM mainboard). Details of the real-time digital signal processing have been described previously (Zrenner et al., 2018).

A multirate real-time model was programmed to process sliding windows of data at a fixed fundamental sample time step size of 0.5 ms. The sliding window was configured to have a length of 1000 samples (500 ms). The real-time system could be configured to trigger TMS pulses in a predetermined sequence or, in accordance with EEG power and phase of the acquired analog EEG signal, at either the EEG-positive or EEG-negative peak of the μ-rhythm as determined by the spatially filtered C3 and C4 electrode EEG signals. The parameters and execution of the real-time system were asynchronously controlled from a standard PC running Microsoft Windows 8 and The MathWorks MATLAB R2016a through an Ethernet connection. The sequence and timing of TMS triggering were controlled from a separate room through a customized automatic script.

Real-time μ-phase-dependent dual-site brain stimulation. The Hjorth-C3 and Hjorth-C4 signals were used for estimation of power and phase. To estimate instantaneous phase at the edge of the sliding window ("time 0"), an autoregressive forward prediction method for Hjorth-C3 and Hjorth-C4 signals was implemented (Chen et al., 2013). The sliding window was zero-phase forward and backward filtered using an FIR 8–12 Hz band-pass filter. The backward filtering step is part of a more general implementation that allows for use of IIR filters. When using FIR filters, it would be simpler to implement an equivalent phase detection algorithm more efficiently without the backward filtering step. Next, it was trimmed by 64 ms segments on both ends to reduce edge effects and the remaining 372 ms signal segment was used to generate the coefficients for

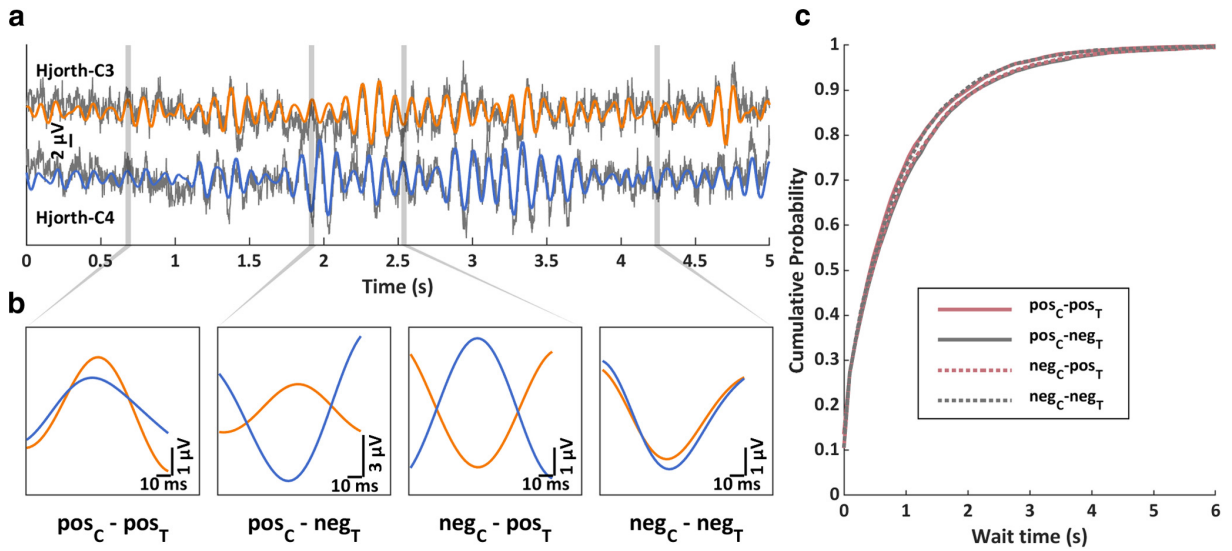

Figure 2. Frequency of occurrence of interhemispheric μ-phase conditions in nonstimulated resting-state EEG. ***a***, Five seconds of scalp raw resting-state EEG recordings (gray traces, top: Hjorth-C3, bottom: Hjorth-C4) for one exemplary subject and corresponding μ-band (8–12 Hz) filtered signals (orange and blue traces, respectively). Vertical shaded gray bars highlight four events corresponding to the four combinations of positive (pos) and negative (neg) peak of the ongoing sensorimotor μ-rhythm in the conditioning (C) and the test (T) M1 (pos_C-pos_T, pos_C-neg_T, neg_C-pos_T, neg_C-neg_T) used for triggering of TMS pulses in the main experiment to determine effects of phase on short-interval interhemispheric inhibition. ***b***, Enlargement of the events highlighted by the vertical gray bars in ***a***. ***c***, Group average ($n = 16$) empirical cumulative probability distributions of waiting time between the occurrence of an event and the next occurrence of the same event for the 4 phase combinations in 5 min of spontaneous resting-state EEG.

an autoregressive forward prediction model (Yule–Walker, order 30), which served to iteratively compute a forecast 128 ms into the future ±64 ms around "time 0" (Zrenner et al., 2018). Instantaneous phase was estimated by calculating the analytic signal from the 128 ms window using a Hilbert transform. Simultaneously, the power spectra of the Hjorth-C3 and Hjorth-C4 signals were calculated from the entire sliding window using an autoregressive Yule–Walker model with order 200 to optimize spectral resolution in the μ-frequency band (8–12 Hz) (McFarland and Wolpaw, 2008). A TTL signal was generated to trigger the magnetic stimulator when the signal reached the target phase and a predetermined μ-power threshold was exceeded. The μ-power threshold was common for the Hjorth-C3 and Hjorth-C4 signals and ensured that the phase estimation was performed on physiological μ-oscillation and not filtered noise. It was set manually at the beginning of the experiment and, if necessary, adjusted during the experiment to keep the intertrial interval between 2 and 4 s. As we have reported previously (Zrenner et al., 2018), the phase prediction algorithm is highly accurate on average, but has an SD of ~50° over all trials. This variability is explained by the approach of forward-predicting a band-pass-filtered signal that requires a trade-off between the efficacy of the filter and the length of the prediction interval.

Experimental sessions. The experiment started with recording 5 min of resting-state EEG (eyes open, subjects instructed to relax and watch at a fixation cross at eye level 1 m in front of them) (Fig. 2).

Next, single-pulse TMS was delivered to the motor hotspots of the left and right M1 to determine RMT and SI_{1mV}. RMT was determined to the nearest 1% of MSO and defined as the minimum intensity that elicited MEPs ≥50 μV peak-to-peak amplitude in at least five of 10 consecutive trials (Groppa et al., 2012). SIHI from the left M1 to the right M1 was probed with a paired-pulse TMS paradigm with a suprathreshold CS delivered to the left M1, followed by a suprathreshold TS delivered to the right M1 at individualized delays of 10 ms ($n = 8$ subjects) or 12 ms ($n = 8$ subjects) (Ferbert et al., 1992) (Fig. 1*d*). These ISIs were chosen because they consistently lead to SIHI (Ferbert et al., 1992; Daskalakis et al., 2002). In the first six subjects, the ISI of 10 ms was tested first and, if not producing sufficient SIHI to meet the inclusion criterion (percentage of conditioned over unconditioned MEP ≤90% for at least one of the CS intensities, see below), the ISI of 12 ms was tested. In the following 10 subjects, the ISI of 12 ms was tested first and then 10 ms later if SIHI with ISI of 12 ms did not meet the inclusion criterion. CS was always applied over the left M1 because all subjects were right-handed and previous studies have shown that SIHI is stronger and more consistently expressed when conditioning the dominant left rather than the nondominant right M1 in right-handers (Netz et al., 1995; Kobayashi et al., 2003). In the SIHI measurements, one target muscle (either APB or FDI) was selected to define TS and CS intensities: the one with lower RMT in the right M1 or the FDI in case of equal RMTs (ABP: 5/16 subjects, FDI: 11/16 subjects). The intensity for the TS over the right M1 was adjusted to produce ~1 mV MEP peak-to-peak amplitude in the left-hand target muscle (when TS was given alone). To select the intensity of the CS, SIHI curves were obtained, where a CS of varying intensity (six different intensities, 90–140% of RMT, in steps of 10% RMT) preceded the TS. Ten conditioned MEPs were collected for each CS intensity, along with 10 unconditioned MEPs (i.e., TS was given alone) in randomized order. The peak-to-peak amplitudes of the conditioned MEPs were averaged for the different CS intensities and then expressed as a percentage of the mean unconditioned MEP amplitude. SIHI intensity curves were plotted (Fig. 3) and a CS intensity that corresponded to the steep, "nonsaturated" part of the SIHI curve was chosen for the main experiment. This procedure ensured for each subject that SIHI was approximately half-maximum and sensitive to assess possible effects of μ-oscillation phase in the main experiment.

Thereafter, the main SIHI experiment with paired-pulse TMS was performed in four experimental blocks (~250 trials each) with fixed ISI, CS, and TS intensity. Within each block, five trigger conditions were tested, with equal numbers of paired pulses and unconditioned test pulses for either one of the following conditions. Trigger conditions (Fig. 1*c*) corresponded to the four possible combinations of positive (pos) and negative (neg) peaks of the ongoing sensorimotor μ-rhythm in the conditioning (C) left M1 and the test (T) right M1: pos_C-pos_T, pos_C-neg_T, neg_C-pos_T, neg_C-neg_T. A random phase condition ($rand_{C/T}$) served as control. The random phase trigger condition used the same 8–12 Hz power threshold criterion as the phase-triggered conditions, but, instead of requiring a positive or negative peak phase detection event to occur, the stimulators were automatically triggered after a uniformly random delay between 0 and 100 ms. The five conditions were tested in random-

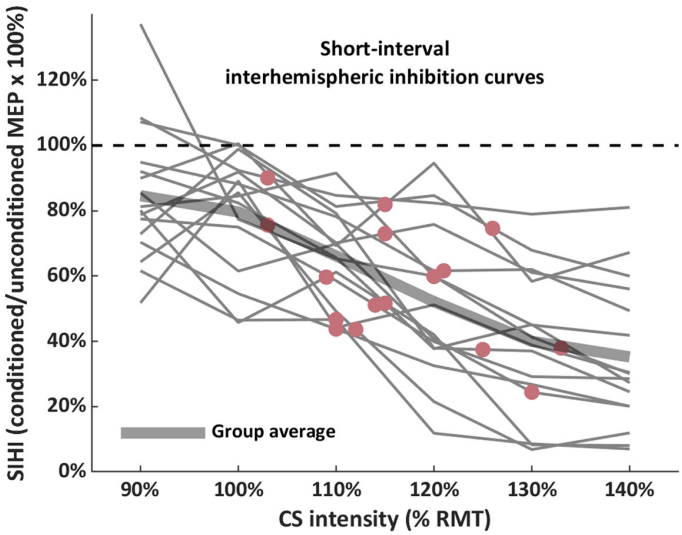

Figure 3. SIHI curves. The SIHI curves of the individual subjects are represented with thin gray lines. SIHI (*y*-axis) is expressed as a percentage of the mean conditioned MEP over the mean unconditioned test MEP and plotted against CS intensity (*x*-axis, in %RMT). The CS preceded the test stimulus by 10 ms in 8/16 subjects and by 12 ms in 8/16 subjects. The red dots superimposed to the individual curves represent the CS intensity selected for the main experiment. For each subject, CS intensity was selected to induce on average ~50% of maximum inhibition. The thick gray line represents the group mean SIHI curve of the studied sample.

ized order with a minimum intertrial interval of 2 s and a total of ~200 trials/condition. The mean intertrial interval (±1 SD) was 3.3 ± 0.3 s and a one-way repeated measure ANOVA (rmANOVA) revealed no difference of mean intertrial intervals between the 4 specific phase conditions ($F_{(1.48,22.23)} = 0.36$, $p = 0.64$, $\eta_p^2 = 0.02$).

Data analysis. The 5 min of resting-state nonstimulated EEG were spatially filtered in each subject to obtain the Hjorth-C3 and Hjorth-C4 signals. Next, these signals were μ-band (8–12 Hz) filtered and instantaneous phase was estimated taking the phase of the analytic signal obtained with a Hilbert transform. Events of interest (pos_C-pos_T, pos_C-neg_T, neg_C-pos_T, neg_C-neg_T) were marked (with a phase tolerance of ±¼ π). The waiting time for a particular event was then analyzed as the occurrence of this event and the next occurrence of the same event for each of the 4 events of interest in the 5 min of resting-state EEG. A rmANOVA revealed that there was no difference between events of interest for the waiting time at 50% cumulative probability ($F_{(1.07,16.11)} = 0.54$, $p = 0.49$; $\eta_p^2 = 0.04$; pos_C-pos_T: 0.43 ± 0.14 s, pos_C-neg_T: 0.48 ± 0.17 s, neg_C-pos_T: 0.47 ± 0.14 s, neg_C-neg_T: 0.44 ± 0.13 s) (Fig. 2*c*). Another rmANOVA demonstrated that also the likelihood of occurrence was not different between the 4 events of interest ($F_{(1.01,15.15)} = 0.91$, $p = 0.36$, $\eta_p^2 = 0.06$; pos_C-pos_T: 26.2 ± 4.5%, pos_C-neg_T: 23.9 ± 4.5%, neg_C-pos_T: 24.0 ± 4.3%, neg_C-neg_T: 26.0 ± 4.3%).

EMG and EEG data processing for the main experiment was performed using the Fieldtrip open source toolbox (Oostenveld et al., 2011) and customized analysis scripts on MATLAB (The MathWorks, R2016a, RRID:SCR_001622). EMG signals were zero-phase band-pass filtered (20–500 Hz) with a third-order Butterworth filter and an additional third order zero-phase Butterworth notch filter (49–51 Hz) to reduce power line noise. Trials contaminated by involuntary muscle contraction in the 500 ms period before the TMS pulse were discarded (mean ±1 SD: 5.2 ± 2.2% of all trials) because preinnervation increases MEP amplitude (Hallett, 2007). Single-trial peak-to-peak MEP amplitudes were automatically determined in the remaining trials within 20–45 ms after the TMS pulse.

For the EEG analysis, the continuous EEG signal was first segmented into epochs from 500 to 1 ms before the CS marker (prestimulation period). Next, manual artifact rejection was performed. Epochs with artifacts in one or more channels were discarded (mean ±1 SD: 6.5 ± 4.2% of all epochs). Single channels with artifact contamination in the majority of epochs were removed (mean ±1 SD: 4 ± 2). Independent component analysis (ICA) based on a FastICA decomposition algorithm with a symmetric approach and the "Gauss" contrast function for finding the weight of matrix was applied (Hyvärinen et al., 2010). The resulting ICA components were visually inspected for topography, single-trial time course, average time course, and power spectrum. Components representing eye blinking, eye movements, and heartbeat were removed. After ICA cleaning, removed channels were spline interpolated using the signals of the neighboring channels (Perrin et al., 1989). EEG signals were then re-referenced to an average reference montage. Analysis of the origin of the Hjorth-C3 and Hjorth-C4 signals was provided in CSD topographical plots (Fig. 4). This corroborated that the positive and negative peaks of the EEG signal used for TMS triggering were specifically localized over the left and right hemispheric sensorimotor cortices.

After the experiment, the resting-state EEG data were fed into the real-time system and triggers for the five trigger conditions were set in the data. These nonstimulated trials were used to determine the actual phase on the Hjorth-C3 signal at the time of the CS trigger and on the Hjorth-C4 signal at the time of the TS trigger and thus to assess the accuracy of the real-time system (rose plots in Fig. 4).

Experimental design and statistical analysis. Statistical analyses were performed with IBM SPSS Statistics version 23 (RRID:SCR_002865). Distribution of data was checked with the Shapiro–Wilk test. All data were normally distributed ($p > 0.05$) and therefore analyzed with parametric tests. SIHI was defined as the percentage of the mean conditioned MEP amplitude over mean unconditioned MEP amplitude (SIHI = conditioned MEP/unconditioned MEP × 100%); that is, smaller SIHI values represent stronger inhibition. The effects of μ-oscillation phase conditions on test MEP amplitude, conditioning MEP amplitude, and SIHI were tested using two-way rmANOVA with the within-subject effects of PHASE (5 levels: pos_C-pos_T, pos_C-neg_T, neg_C-pos_T, neg_C-neg_T, $rand_{C/T}$) and MUSCLE (2 levels: APB, FDI). To disentangle effects of phase synchronicity (SYNC) from effects of local excitability in the conditioning left M1 and test right M1, another rmANOVA with the within-subject effects of SYNC (two levels: in phase (neg_C-neg_T, pos_C-pos_T) versus out of phase (neg_C-pos_T, pos_C-neg_T), PHASE in test M1 (two levels: negative peak versus positive peak) and MUSCLE (two levels: APB, FDI) was performed. The SYNC × PHASE in test M1 interaction represents the effect of PHASE in the conditioning M1. Mauchly's test examined sphericity and, in case of violation of sphericity, the Greenhouse–Geisser correction of degrees of freedom was applied. *Post hoc* paired two-tailed *t* tests were applied whenever main effects or their interactions were significant. The significance level for all statistical tests was set to $p < 0.05$. Data are given as means ±1 SEM unless indicated otherwise.

Results

All procedures were well tolerated and no adverse events were noted. TMS measures are presented as means ±1 SEM.

The CSD plots of the EEG signal in the 20 ms preceding the trigger showed a highly localized positivity/negativity over the left and right M1 regions in all phase-specific trigger conditions, with almost no contamination by occipital alpha (Fig. 4). This suggested that the Hjorth-C3 and Hjorth-C4 EEG signal that was used for triggering the TMS pulses originated predominantly from the stimulated primary sensorimotor cortices.

The full design for testing SIHI is illustrated in Figure 1. It involved five PHASE conditions (Fig. 1*c*) and single-pulse TMS of the test M1 (right M1) and recording of associated muscle

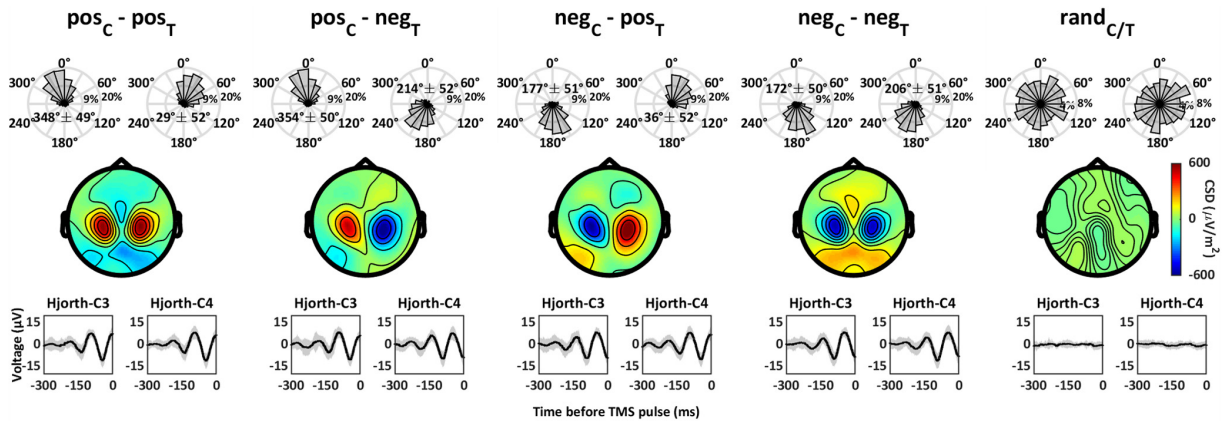

Figure 4. SIHI triggered on the instantaneous phase of sensorimotor μ-oscillation over left and right motor cortex. Top, Distribution of estimated phase angle at the time of the CS trigger for the conditioning motor cortex (left M1, left in each pair of rose plots) and TS trigger (10 or 12 ms later) for the test motor cortex (right M1, right) in triggered nonstimulated resting-state trials in the five different phase trigger conditions, indicated in the headers. Phase angles are binned (width, 18°) and frequencies are indicated (inner ring = 9%, outer ring = 20% for all phase-specific conditions, inner ring = 4%, outer ring = 8% for the random phase condition). Angular means ±1 SD are indicated in the phase distribution plots for all phase-specific conditions. Middle, Group mean CSD plots in the 20 ms preceding TMS. Amplitudes (in $\mu V/m^2$) are indicated by the color bar. Bottom, Grand averages across all subjects and trials of raw sensorimotor Hjorth-C3 and Hjorth-C4 EEG signals preceding the TMS pulse at 0 ms. Shadings represent ±1 SD physiological shifts in μ-oscillation frequency across different trials and individuals are responsible for the declining oscillation amplitudes with distance to the TMS pulse.

responses (MEP), providing a reference measure (Fig. 1*d*, left hand: unconditioned MEP = dashed line) for comparison with dual-coil, paired-pulse TMS, where a conditioning TMS pulse of the conditioning M1 (left M1) precedes the right M1 test pulse by 10–12 ms (Fig. 1*d*, left hand: conditioned MEP = solid line). Importantly, the conditioning pulse was also suprathreshold, evoking MEPs (Fig. 1*d*, right hand: conditioning MEP = solid line). SIHI was expressed as the ratio of conditioned over unconditioned MEP amplitude in the left hand. The three measures (unconditioned MEP, conditioning MEP, and SIHI) allowed to infer to what extent SIHI, the measure of effective interhemispheric connectivity, covaried with interhemispheric PHASE relations and PHASE-dependent variation of local excitability in the conditioning and test M1. The following sections report the findings on these three measures.

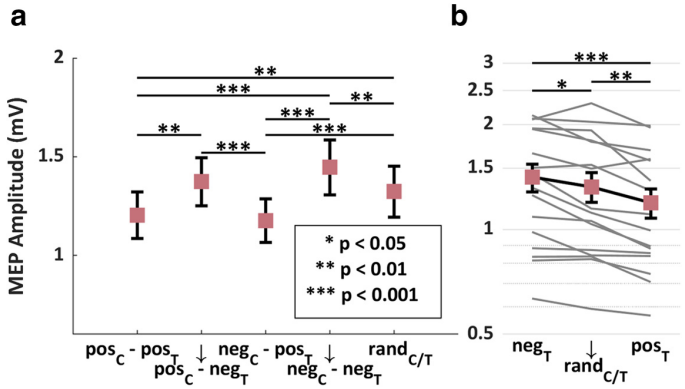

Figure 5. Effect of phase of μ-rhythm on unconditioned test MEP amplitude. ***a***, Mean ($n = 16$) ±1 SEM unconditioned test MEP amplitudes (*y*-axis, mean MEP amplitudes in mV) evoked by the test stimulus alone applied to right test M1 in the 5 different phase conditions (*x*-axis). Data are pooled over the two target muscles (APB, FDI). ***b***, Individual MEP data (in millivolts, logarithmic scale, *y*-axis). Data have been merged according to the phase in test M1. MEP amplitude is larger at the negative peak versus positive peak condition in all subjects, with intermediate MEP amplitudes in the random phase condition in 12/16 subjects. $^*p < 0.05$, $^{**}p < 0.01$, $^{***}p < 0.001$.

Effect of phase of μ-rhythm on unconditioned test MEP amplitude

rmANOVA showed a significant effect of PHASE ($F_{(4,60)} = 12.53$, $p < 0.001$, $\eta_p^2 = 0.46$), but no effects of MUSCLE ($F_{(1,15)} = 0.52$, $p = 0.48$, $\eta_p^2 = 0.03$) or the PHASE × MUSCLE interaction ($F_{(1.79,26.80)} = 0.54$, $p = 0.71$, $\eta_p^2 = 0.04$). The mean unconditioned test MEP amplitudes (±1 SEM) pooled across the two target muscles were as follows: pos_C-pos_T: 1.20 ± 0.11 mV, pos_C-neg_T: 1.37 ± 0.12 mV, neg_C-pos_T: 1.18 ± 0.10 mV, neg_C-neg_T: 1.45 ± 0.14 mV, $rand_{C/T}$: 1.32 ± 0.12 mV (Fig. 5). *Post hoc* two-tailed paired *t* tests showed several significant pairwise differences as indicated in Figure 5.

The data replicate previous findings (Zrenner et al., 2018) by showing that MEPs are larger when the test M1 is stimulated at the negative peak of the μ-rhythm compared with the positive peak, with intermediate MEP amplitudes in the random phase condition.

Effect of phase of μ-rhythm on conditioning MEP amplitude

rmANOVA showed a significant effect of PHASE ($F_{(4,60)} = 4.10$, $p = 0.005$, $\eta_p^2 = 0.22$), but no effect of MUSCLE ($F_{(1,15)} = 0.66$, $p = 0.43$, $\eta_p^2 = 0.04$) or the PHASE × MUSCLE interaction ($F_{(2.66,39.93)} = 0.49$, $p = 0.67$, $\eta_p^2 = 0.03$).

Mean conditioning MEP amplitudes (±1 SEM) pooled across the two target muscles were as follows: pos_C-pos_T: 0.93 ± 0.12 mV, pos_C-neg_T: 0.94 ± 0.13 mV, neg_C-pos_T: 1.05 ± 0.13 mV, neg_C-neg_T: 0.99 ± 0.12 mV, $rand_{C/T}$: 1.01 ± 0.13 mV (Fig. 6). *Post hoc* two-tailed paired *t* tests showed several significant pairwise differences as indicated in Figure 6. In particular, the neg_C-pos_T condition, that is, when the conditioning left M1 is stimulated at the negative peak of the μ-rhythm, revealed larger MEPs than most of the other conditions. The weaker effect of

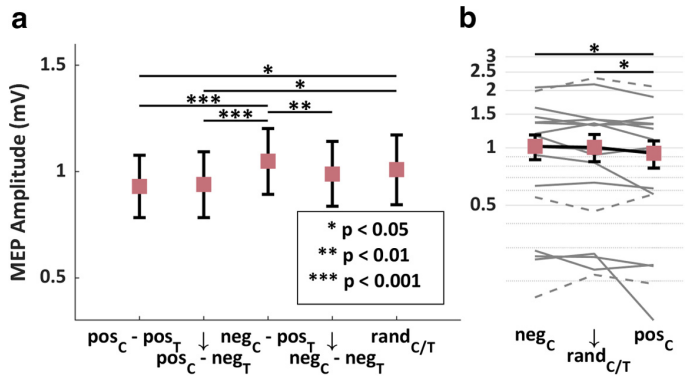

Figure 6. Effect of phase of μ-rhythm on conditioning MEP amplitude. ***a***, Mean ($n = 16$) ±1 SEM unconditioned test MEP amplitudes (*y*-axis, mean MEP amplitudes in mV) evoked by the conditioning stimulus applied to left M1 in the 5 different phase conditions (*x*-axis). Data are pooled over the two target muscles (APB, FDI). ***b***, Individual MEP data (in millivolts, logarithmic scale, *y*-axis). Data have been merged according to the phase in conditioning M1. MEP amplitude is larger at the negative peak versus positive peak condition in 13/16 subjects. $^*p < 0.05$, $^{**}p < 0.01$, $^{***}p < 0.001$.

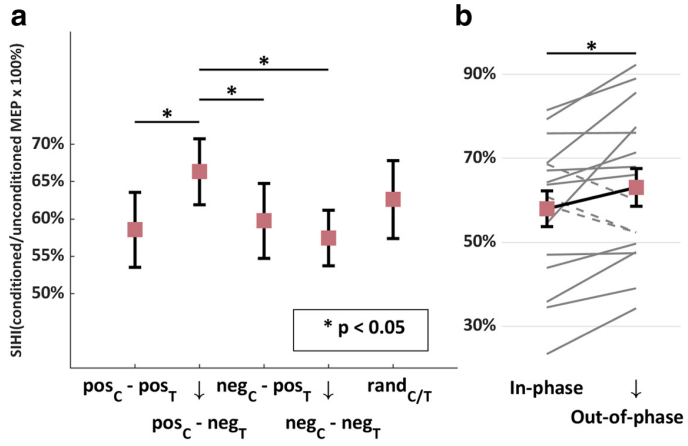

Figure 7. Effect of phase of μ-rhythm on SIHI. ***a***, Mean ($n = 16$) ±1 SEM SIHI (*y*-axis) expressed as a percentage of the mean conditioned MEP over the mean unconditioned test MEP and is shown for the five phase conditions (*y*-axis). Data are pooled over the two target muscles (APB, FDI). ***b***, Individual SIHI data (as a percentage, *y*-axis). Data have been merged for in-phase (pos_C-pos_T, neg_C-neg_T) versus out-of-phase (pos_C-neg_T, neg_C-pos_T) conditions. SIHI is stronger in the in phase condition in 13/16 subjects. $^*p < 0.05$.

PHASE on conditioning MEP amplitude compared with test MEP amplitude may have been caused by the necessary adjustments of location and rotation of the conditioning stimulating coil (see Materials and Methods) because previous data showed this to be critical for the effect size of the PHASE effect (see Fig. 5 in Zrenner et al., 2018).

Effect of phase of μ-rhythm on SIHI

rmANOVA showed a strong effect of PHASE ($F_{(4,60)} = 3.02$, $p = 0.024$, $\eta_p^2 = 0.17$), but no effect of MUSCLE ($F_{(1,15)} = 0.26$, $p = 0.62$, $\eta_p^2 = 0.02$) or PHASE × MUSCLE interaction ($F_{(4,60)} = 0.80$, $p = 0.53$, $\eta_p^2 = 0.05$) on SIHI.

Mean SIHI (±1 SEM) pooled across the two target muscles was as follows: pos_C-pos_T: 59 ± 5%, pos_C-neg_T: 66 ± 4%, neg_C-pos_T: 60 ± 5%, neg_C-neg_T: 57 ± 4%, $rand_{C/T}$: 63 ± 5% (Fig. 7). *Post hoc* two-tailed paired *t* tests showed significant pairwise differences as indicated in Figure 7.

These data suggest a relevant role of local excitability in the conditioning and test M1, resulting in least SIHI in the pos_C-neg_T, that is, when conditioning MEP amplitude is small (cf. Fig. 6) and unconditioned test MEP amplitude is large (cf. Fig. 5).

Previous studies have shown that SIHI increases with increasing conditioning MEP amplitude (Ferbert et al., 1992; Ni et al., 2009; Ghosh et al., 2013), but decreases with increasing test MEP amplitude (Ferbert et al., 1992; Daskalakis et al., 2002).

To disentangle the role of phase synchrony (SYNC) from effects of local PHASE in the conditioning and test M1, we performed a rmANOVA with the within-subject effects of SYNC (two levels: in phase vs out of phase), PHASE in the test M1 (two levels: negative peak vs positive peak), and MUSCLE (two levels: APB, FDI). The SYNC × PHASE in the test M1 interaction represents the effect of PHASE in the conditioning M1.

The rmANOVA showed significant effects of SYNC ($F_{(1,15)} = 5.16$, $p = 0.038$, $\eta_p^2 = 0.26$) and PHASE in the conditioning M1 ($F_{(1,15)} = 5.41$, $p = 0.034$, $\eta_p^2 = 0.27$), but no effect of PHASE in the test M1 ($F_{(1,15)} = 1.47$, $p = 0.25$, $\eta_p^2 = 0.09$), MUSCLE ($F_{(1,15)} = 0.29$, $p = 0.60$, $\eta_p^2 = 0.02$) or interactions of MUSCLE with any of the other effects (all $p > 0.2$, all $\eta_p^2 < 0.1$). Stronger effective connectivity (i.e., smaller values of SIHI) occurred in the in phase compared with out of phase conditions and in the conditioning M1 high-excitability state (i.e., negative peak of the μ-rhythm in the conditioning M1) (Fig. 7).

To rule out that the duration of the synchronized state before the TMS pulse has contributed to the observed SIHI effects, we estimated the phase-locking value (PLV) over the 500 ms preceding TMS (Lachaux et al., 1999). We used the Hilbert transform preceded by singular spectrum decomposition (SSD) of the signal, as described previously (Lowet et al., 2016). The SSD component representing the μ-rhythm was automatically identified by estimating the power spectrum of each resulting component and selecting the component with the largest peak in the 5–15 Hz frequency band. This approach isolated the μ-oscillation minimizing the loss of signal at the edges due to bandpass filtering and Hilbert transform. The resulting PLV between the Hjorth-C3 and Hjorth-C4 signals in the μ-phase-triggered conditions is reported in Figure 8. The PLV time course is virtually identical across conditions, ruling out the possibility that there were different durations of the pre-TMS synchronization between the Hjorth-C3 and Hjorth-C4 signals between the different PHASE conditions.

Discussion

The extent to which interhemispheric communication can be predicted by phase relations of ongoing oscillations in the human sensorimotor cortex is thus far unknown because electrophysio-

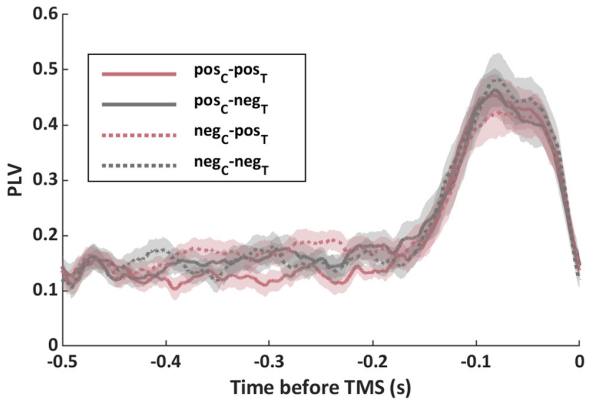

Figure 8. Time course of the PLV between the Hjorth-C3 and Hjorth-C4 signals before TMS for the 4 μ-phase trigger conditions (group average ±1 SEM, $n = 16$). The PLV shows a very similar pattern across conditions, ruling out the possibility that different durations of the pre-TMS synchronization between the trigger signals across the different μ-phase conditions may have played a role in the obtained SIHI results. For the time points close to TMS (up to ~−40 ms), PLV estimation is distorted by the edge effect of the Hilbert transform used to estimate the phase of the μ-oscillation.

logical studies investigating interhemispheric sensorimotor interactions have disregarded the continuously fluctuating brain dynamics. We report here first findings in healthy human subjects in whom SIHI, a marker of effective inhibitory interhemispheric motor connectivity, was investigated with dual-site millisecond-resolved brain-state-dependent EEG-triggered TMS based on the instantaneous phase of the sensorimotor μ-rhythm in the two hemispheres. Instantaneous phase relation of the Hjorth-C3 and Hjorth-C4 signals from the sensorimotor cortices of the two hemispheres continuously fluctuates between in phase and out of phase conditions (Fig. 2), similar to incessantly varying phase correlations in bihemispheric M1 local field potential recordings (Murthy and Fetz, 1996).

Consistent with previous open-loop paired-coil TMS studies that demonstrated an increase of SIHI with increasing conditioning MEP amplitude (Ferbert et al., 1992; Ni et al., 2009; Ghosh et al., 2013), our findings show effects of local excitability in the conditioning M1; that is, stronger SIHI when the conditioning M1 is stimulated in the high-excitability state (negative peak of the μ-rhythm) (Fig. 7). Importantly, our findings also demonstrate for the first time a significant effect of interhemispheric μ-phase synchronicity, with stronger SIHI in the in phase than out of phase conditions (Fig. 7). These findings are predicted by the CTC theory (Fries, 2005, 2015) and experimental evidence from multiunit recordings in cat and monkey visual cortex (Womelsdorf et al., 2007).

Negative deflections in the surface EEG reflect synchronized EPSCs at the apical dendrites of radially oriented pyramidal cells (Buzsáki et al., 2012). TMS is thought to activate motor output neurons in M1 predominantly transsynaptically by excitation of long-range corticocortical axons at the precentral and postcentral gyrus crowns where the TMS-induced electrical fields are maximal (Laakso et al., 2014; Bungert et al., 2017; Laakso et al., 2018). Accordingly, excitation through the TMS pulse given at the time of the negative peak of the sensorimotor μ-rhythm will add to the elevated firing rate of neurons in premotor and somatosensory cortex that are projecting to M1 (Haegens et al., 2011) and this will lead to recruitment of a larger fraction of corticospinal neurons in M1, as indexed by the larger MEP amplitude (Figs. 5, 6) (Zrenner et al., 2018). Long-range corticocortical axons from somatosensory cortex terminate in monkey Brodmann area 4 (primary motor cortex) in cortical layers V and III (DeFelipe et al., 1986), where the corticospinal cells and transcallosal projection cells to the opposite M1 are located, respectively (Jones and Wise, 1977). Therefore, it is likely that the excitability states of corticospinal cells and transcallosal projection cells are co-modulated as a function of μ-rhythm phase. Furthermore, previous SIHI experiments demonstrated that conditioning MEP amplitude and SIHI are directly related (Ni et al., 2009; Ghosh et al., 2013). SIHI is very likely mediated through motor callosal fibers connecting the hand areas of the two M1 because there is a direct correlation of SIHI magnitude with microstructural integrity of these fibers as measured by diffusion tensor imaging (Wahl et al., 2007). The transcallosal connection is excitatory (glutamatergic) and inhibition is mediated by termination of this connection on inhibitory interneurons in the opposite M1 (Innocenti, 1986). These interneurons receive long-range excitatory input from other sources such as somatosensory cortex (Markram et al., 2004). This anatomical circuitry predicts that, at the negative peak of the μ-rhythm, the SIHI-mediating inhibitory interneurons in the test M1 will be in a state of high sensitivity to excitatory synaptic input (e.g., from the transcallosal projection neurons) because they are then depolarized by the elevated input from somatosensory cortex. Together with maximal spike output of transcallosal projection neurons in the conditioning M1, this would explain why maximal SIHI was obtained when both M1 were phase synchronized at the negative peak of the μ-rhythm, as predicted by the CTC theory.

The present findings are also consistent with noninvasive brain stimulation experiments that investigated the consequences on SIHI after altering corticospinal excitability. One-Hertz repetitive TMS over the conditioning M1 resulted in increased corticospinal excitability of the nonstimulated test M1 and/or decreased excitability of the conditioning M1, in parallel with a decrease in SIHI (Gilio et al., 2003; Pal et al., 2005). Similarly, transcranial direct current stimulation of bilateral M1 resulted in deceased corticospinal excitability under the cathode, increased excitability under the anode, and decreased SIHI from the less excitable M1 to the more excitable M1 and, vice versa, increased SIHI when testing from the more to less excitable M1 (Tazoe et al., 2014).

Furthermore, this conceptual background also explains why we found weakest SIHI when the conditioning M1 was in the low-excitability state at the positive peak of the μ-rhythm and out of phase with the test M1 in the high-excitability state. The reverse out-of-phase condition (conditioning M1 in high-excitable state, test M1 in low-excitable state) resulted in stronger SIHI (Fig. 7).

Finally, our findings have a potentially important translational perspective. We showed previously that single-site repetitive burst stimulation at the high-excitability state of the sensorimotor cortex resulted in long-term potentiation-like increase in corticospinal excitability, but not when applying the same repetitive stimulation at the low-excitability state (Zrenner et al., 2018). It might be expected that, in conjunction with the CTC theory and the principle of cooperativity for induction of synaptic plasticity (Sjöström et al., 2001), dual-site repetitive TMS of the two M1 at instances of phase synchrony for the high-excitability state will be most successful in modifying interhemispheric effective connectivity as expressed by SIHI than any of the other states that have been tested in the present experiments. SIHI from contralesional to ipsilesional M1 is exaggerated in the

early phase after stroke (Boddington and Reynolds, 2017) and current approaches of therapeutic brain stimulation are targeting this abnormality by downregulating corticospinal excitability in the contralesional M1 with moderate effect size (Grefkes et al., 2010; Avenanti et al., 2012).

This study has several limitations. First, we cannot be certain that the fluctuating synchronization of the μ-rhythm in the sensorimotor cortices of the two hemispheres is mediated through the corpus callosum. Although oscillatory synchrony across hemispheres is considered predominantly mediated by transcallosal connections in visual cortex (Engel et al., 1991), a significant contribution of a common modulatory drive from subcortical regions such as the thalamus cannot be excluded (Vijayan and Kopell, 2012). However, this is not critical for the interpretation of the present findings because there is strong evidence that SIHI, the outcome measure of this study, is largely, if not exclusively, mediated through motor callosal fibers (see above). Second, it is not certain that the EEG oscillations that were used for TMS triggering were generated by the sensorimotor μ-rhythm and not by another sensorimotor rhythmic activity in the alpha-frequency band that shows increased interhemispheric coherence during voluntary unilateral index finger movements (Florian et al., 1998). However, we have confirmed during screening that the Hjorth-3 and Hjorth-C4 sensorimotor oscillations in the alpha-frequency range desynchronized in all subjects with fist clenching, an accepted criterion for μ-rhythm identification (Chatrian et al., 1959; Salenius et al., 1997). Furthermore, there was no relevant contribution from the occipital alpha-rhythm, as can be noted from the focal CSD potentials over the sensorimotor cortices and absence of dipoles over the occipital cortex (Fig. 4). Third, we have not tested the CTC hypothesis for oscillations in other frequency bands. In particular, oscillations in the beta-frequency band (13–30 Hz) play important roles in human sensorimotor cortex, for example, during maintenance of tonic motor output or at rest (Pfurtscheller and Lopes da Silva, 1999; Baker, 2007). Furthermore, interhemispheric synchronization during bimanual and unimanual motor tasks was observed in monkey motor cortex for activity in the beta-frequency band (Murthy and Fetz, 1996). Therefore, future experiments should test the effects of interhemispheric phase synchronization of sensorimotor beta-oscillations on SIHI during rest and motor tasks. Fourth, slight repositioning and reorienting of the conditioning coil was necessary in most of the subjects to fit both coils tangentially on the scalp. This likely explained the moderated μ-phase-dependent effect on conditioning compared with test MEP amplitude (see Results), but may also have led to a suboptimal performance and thus underestimation with respect to μ-phase modulation of SIHI. Future experiments could use smaller stimulating coils to address this issue.

In conclusion, this EEG-TMS study demonstrates that interhemispheric phase synchronicity of the two sensorimotor cortices at the negative peak of the endogenous μ-rhythm, a high-excitability state, was associated with optimal effective interhemispheric motor connectivity, as indexed by maximal short-interval interhemispheric inhibition measured in a paired-coil TMS protocol. Our findings support the notion that temporal dynamics of neuronal oscillations in reciprocal neuronal networks significantly affect large-scale interhemispheric network communication, consistent with the theory of communication through coherence.

References

Avenanti A, Coccia M, Ladavas E, Provinciali L, Ceravolo MG (2012) Low-frequency rTMS promotes use-dependent motor plasticity in chronic stroke: a randomized trial. Neurology 78:256–264. CrossRef Medline

Baker SN (2007) Oscillatory interactions between sensorimotor cortex and the periphery. Curr Opin Neurobiol 17:649–655. CrossRef Medline

Boddington LJ, Reynolds JNJ (2017) Targeting interhemispheric inhibition with neuromodulation to enhance stroke rehabilitation. Brain Stimul 10: 214–222. CrossRef Medline

Bungert A, Antunes A, Espenhahn S, Thielscher A (2017) Where does TMS stimulate the motor cortex? Combining electrophysiological measurements and realistic field estimates to reveal the affected cortex position. Cereb Cortex 27:5083–5094. CrossRef Medline

Buzsáki G, Draguhn A (2004) Neuronal oscillations in cortical networks. Science 304:1926–1929. CrossRef Medline

Buzsáki G, Anastassiou CA, Koch C (2012) The origin of extracellular fields and currents–EEG, ECoG, LFP and spikes. Nat Rev Neurosci 13:407–420. CrossRef Medline

Chatrian GE, Petersen MC, Lazarte JA (1959) The blocking of the rolandic wicket rhythm and some central changes related to movement. Electroencephalogr Clin Neurophysiol 11:497–510. CrossRef Medline

Chen LL, Madhavan R, Rapoport BI, Anderson WS (2013) Real-time brain oscillation detection and phase-locked stimulation using autoregressive spectral estimation and time-series forward prediction. IEEE Trans Biomed Eng 60:753–762. CrossRef Medline

Daskalakis ZJ, Christensen BK, Fitzgerald PB, Roshan L, Chen R (2002) The mechanisms of interhemispheric inhibition in the human motor cortex. J Physiol 543:317–326. CrossRef Medline

DeFelipe J, Conley M, Jones EG (1986) Long-range focal collateralization of axons arising from corticocortical cells in monkey sensory-motor cortex. J Neurosci 6:3749–3766. CrossRef Medline

Engel AK, König P, Kreiter AK, Singer W (1991) Interhemispheric synchronization of oscillatory neuronal responses in cat visual cortex. Science 252:1177–1179. CrossRef Medline

Ferbert A, Priori A, Rothwell JC, Day BL, Colebatch JG, Marsden CD (1992) Interhemispheric inhibition of the human motor cortex. J Physiol 453: 525–546. CrossRef Medline

Florian G, Andrew C, Pfurtscheller G (1998) Do changes in coherence always reflect changes in functional coupling? Electroencephalogr Clin Neurophysiol 106:87–91. CrossRef Medline

Fries P (2005) A mechanism for cognitive dynamics: neuronal communication through neuronal coherence. Trends Cogn Sci 9:474–480. CrossRef Medline

Fries P (2015) Rhythms for cognition: communication through coherence. Neuron 88:220–235. CrossRef Medline

Ghosh S, Mehta AR, Huang G, Gunraj C, Hoque T, Saha U, Ni Z, Chen R (2013) Short and long-latency inter-hemispheric inhibition are additive in the human motor cortex. J Neurophysiol 109:2955–2962. CrossRef Medline

Gilio F, Rizzo V, Siebner HR, Rothwell JC (2003) Effects on the right motor hand-area excitability produced by low-frequency rTMS over human contralateral homologous cortex. J Physiol 551:563–573. CrossRef Medline

Grefkes C, Nowak DA, Wang LE, Dafotakis M, Eickhoff SB, Fink GR (2010) Modulating cortical connectivity in stroke patients by rTMS assessed with fMRI and dynamic causal modelling. Neuroimage 50:233–242. CrossRef Medline

Groppa S, Oliviero A, Eisen A, Quartarone A, Cohen LG, Mall V, Kaelin-Lang A, Mima T, Rossi S, Thickbroom GW, Rossini PM, Ziemann U, Valls-Solé J, Siebner HR (2012) A practical guide to diagnostic transcranial magnetic stimulation: report of an IFCN committee. Clin Neurophysiol 123: 858–882. CrossRef Medline

Haegens S, Nácher V, Luna R, Romo R, Jensen O (2011) alpha-oscillations in the monkey sensorimotor network influence discrimination performance by rhythmical inhibition of neuronal spiking. Proc Natl Acad Sci U S A 108:19377–19382. CrossRef Medline

Hallett M (2007) Transcranial magnetic stimulation: a primer. Neuron 55: 187–199. CrossRef Medline

Hari R (2006) Action-perception connection and the cortical mu rhythm. Prog Brain Res 159:253–260. CrossRef Medline

Hjorth B (1975) An on-line transformation of EEG scalp potentials into

orthogonal source derivations. Electroencephalogr Clin Neurophysiol 39: 526–530. CrossRef Medline

Hyvärinen A, Ramkumar P, Parkkonen L, Hari R (2010) Independent component analysis of short-time fourier transforms for spontaneous EEG/MEG analysis. Neuroimage 49:257–271. CrossRef Medline

Innocenti GM (1986) General organization of the callosal connections in the cerebral cortex. In: Cerebral cortex (Jones EG, Peters A, eds), pp 291–353. New York: Plenum.

Jensen O, Mazaheri A (2010) Shaping functional architecture by oscillatory alpha activity: gating by inhibition. Front Hum Neurosci 4:186. CrossRef Medline

Jones EG, Wise SP (1977) Size, laminar and columnar distribution of efferent cells in the sensory-motor cortex of monkeys. J Comp Neurol 175: 391–438. CrossRef Medline

Kobayashi M, Hutchinson S, Schlaug G, Pascual-Leone A (2003) Ipsilateral motor cortex activation on functional magnetic resonance imaging during unilateral hand movements is related to interhemispheric interactions. Neuroimage 20:2259–2270. CrossRef Medline

Laakso I, Hirata A, Ugawa Y (2014) Effects of coil orientation on the electric field induced by TMS over the hand motor area. Phys Med Biol 59:203–218. CrossRef Medline

Laakso I, Murakami T, Hirata A, Ugawa Y (2018) Where and what TMS activates: experiments and modeling. Brain Stimul 11:166–174. CrossRef Medline

Lachaux JP, Rodriguez E, Martinerie J, Varela FJ (1999) Measuring phase synchrony in brain signals. Hum Brain Mapp 8:194–208. CrossRef Medline

Lowet E, Roberts MJ, Bonizzi P, Karel J, De Weerd P (2016) Quantifying neural oscillatory synchronization: a comparison between spectral coherence and phase-locking value approaches. PLoS One 11:e0146443. CrossRef Medline

Markram H, Toledo-Rodriguez M, Wang Y, Gupta A, Silberberg G, Wu C (2004) Interneurons of the neocortical inhibitory system. Nat Rev Neurosci 5:793–807. CrossRef Medline

McFarland DJ, Wolpaw JR (2008) Sensorimotor rhythm-based brain-computer interface (BCI): model order selection for autoregressive spectral analysis. J Neural Eng 5:155–162. CrossRef Medline

Murthy VN, Fetz EE (1996) Oscillatory activity in sensorimotor cortex of awake monkeys: synchronization of local field potentials and relation to behavior. J Neurophysiol 76:3949–3967. CrossRef Medline

Netz J, Ziemann U, Hömberg V (1995) Hemispheric asymmetry of transcallosal inhibition in man. Exp Brain Res 104:527–533. Medline

Ni Z, Gunraj C, Nelson AJ, Yeh IJ, Castillo G, Hoque T, Chen R (2009) Two phases of interhemispheric inhibition between motor related cortical areas and the primary motor cortex in human. Cereb Cortex 19:1654–1665. CrossRef Medline

Oostenveld R, Fries P, Maris E, Schoffelen JM (2011) FieldTrip: open source software for advanced analysis of MEG, EEG, and invasive electrophysiological data. Comput Intell Neurosci 2011:156869. CrossRef Medline

Pal PK, Hanajima R, Gunraj CA, Li JY, Wagle-Shukla A, Morgante F, Chen R (2005) Effect of low frequency repetitive transcranial magnetic stimulation on interhemispheric inhibition. J Neurophysiol 94:1668–1675. CrossRef Medline

Perrin F, Pernier J, Bertrand O, Echallier JF (1989) Spherical splines for scalp potential and current density mapping. Electroencephalogr Clin Neurophysiol 72:184–187. CrossRef Medline

Pfurtscheller G, Lopes da Silva FH (1999) Event-related EEG/MEG synchronization and desynchronization: basic principles. Clin Neurophysiol 110:1842–1857. CrossRef Medline

Picazio S, Veniero D, Ponzo V, Caltagirone C, Gross J, Thut G, Koch G (2014) Prefrontal control over motor cortex cycles at beta frequency during movement inhibition. Curr Biol 24:2940–2945. CrossRef Medline

Rossi S, Hallett M, Rossini PM, Pascual-Leone A; Safety of TMS Consensus Group (2009) Safety, ethical considerations, and application guidelines for the use of transcranial magnetic stimulation in clinical practice and research. Clin Neurophysiol 120:2008–2039. CrossRef Medline

Rossini PM et al. (2015) Non-invasive electrical and magnetic stimulation of the brain, spinal cord, roots and peripheral nerves: basic principles and procedures for routine clinical and research application. an updated report from an I.F.C.N. Committee. Clin Neurophysiol 126:1071–1107. CrossRef Medline

Salenius S, Portin K, Kajola M, Salmelin R, Hari R (1997) Cortical control of human motoneuron firing during isometric contraction. J Neurophysiol 77:3401–3405. CrossRef Medline

Seeck M, Koessler L, Bast T, Leijten F, Michel C, Baumgartner C, He B, Beniczky S (2017) The standardized EEG electrode array of the IFCN. Clin Neurophysiol 128:2070–2077. CrossRef Medline

Singer W (1999) Neuronal synchrony: a versatile code for the definition of relations? Neuron 24:49–65, 111–125. CrossRef Medline

Sjöström PJ, Turrigiano GG, Nelson SB (2001) Rate, timing, and cooperativity jointly determine cortical synaptic plasticity. Neuron 32:1149–1164. CrossRef Medline

Tazoe T, Endoh T, Kitamura T, Ogata T (2014) Polarity specific effects of transcranial direct current stimulation on interhemispheric inhibition. PLoS One 9:e114244. CrossRef Medline

Uhlhaas PJ, Singer W (2010) Abnormal neural oscillations and synchrony in schizophrenia. Nat Rev Neurosci 11:100–113. CrossRef Medline

Varela F, Lachaux JP, Rodriguez E, Martinerie J (2001) The brainweb: phase synchronization and large-scale integration. Nat Rev Neurosci 2:229–239. CrossRef Medline

Vijayan S, Kopell NJ (2012) Thalamic model of awake alpha oscillations and implications for stimulus processing. Proc Natl Acad Sci U S A 109: 18553–18558. CrossRef Medline

Wahl M, Lauterbach-Soon B, Hattingen E, Jung P, Singer O, Volz S, Klein JC, Steinmetz H, Ziemann U (2007) Human motor corpus callosum: topography, somatotopy, and link between microstructure and function. J Neurosci 27:12132–12138. CrossRef Medline

Womelsdorf T, Schoffelen JM, Oostenveld R, Singer W, Desimone R, Engel AK, Fries P (2007) Modulation of neuronal interactions through neuronal synchronization. Science 316:1609–1612. CrossRef Medline

Zrenner C, Desideri D, Belardinelli P, Ziemann U (2018) Real-time EEG-defined excitability states determine efficacy of TMS-induced plasticity in human motor cortex. Brain Stimul 11:374–389. CrossRef Medline

4. Discussion

The objectives of this work were threefold. First, we aimed to present the novel method of brain-state-dependent EEG-TMS and provide an experimental pipeline for conduction of EEG-TMS experiments. Second, we assessed whether the μ-rhythm phase dependency of corticospinal excitability is symmetrical across homologous areas of the human primary motor cortices. Third, we investigated the effect of endogenous μ-oscillations with respect to interhemispheric communication between the two primary motor cortices.

In the first paper (Stefanou et al., 2019), we have presented a new method that synchronizes TMS (with a millisecond-resolution) with the endogenous brain oscillations (herein the sensorimotor μ-rhythm), which combined with neuronavigation allows *ad hoc* studies of brain oscillations with a high spatiotemporal precision. We have shown that brain-state dependent EEG-TMS leads to less-variable brain responses and (as shown in previous research (Zrenner et al., 2018a)) to differential plasticity effects. We further argue that the advantages of real-time EEG-TMS render this method a research tool with unique potential, but we also suggest that implementation of this method in therapeutic brain stimulation protocols can enhance the therapeutic efficacy of repetitive TMS (rTMS). First evidence of the therapeutic efficacy of brain-state dependent rTMS over the left dorsolateral prefrontal cortex (DLPFC) as treatment for major depressive disorder have been published in the meantime by our group (Zrenner et al., 2020). Furthermore, application of brain-state dependent rTMS in therapeutic protocols for post-stroke motor recovery comprises a subject of current research. Finally, in the first methodological paper of this thesis (Stefanou et al., 2019), we discussed the technical requirements and challenges of real-time EEG-TMS, along with technical aspects that warrant further optimization and future research (e.g., with respect to implemented algorithms, that extract the desired brain rhythms from recorded EEG signals using spatial and frequency filters).

In the second paper (Stefanou et al., 2020), we used real-time EEG-triggered TMS to study the μ-rhythm phase dependency of corticospinal excitability between the hand-representation areas of the two M1 in 51 right-handed subjects. We found no evidence of interhemispheric asymmetries, as the directionality and effect size of μ-rhythm phase dependency were shown to be similar between the two hemispheres. We concluded, therefore, that despite the presence of well-established functional and anatomical differences between homologous areas in the two M1 (Amunts et al., 2000), the μ-rhythm phase dependency of corticospinal excitability appears to be

a ubiquitous trait of the motor system at rest. In this study, we used resting motor threshold (RMT) as readout of the corticospinal excitability and showed that the negative peak of the μ-rhythm corresponds to a high-excitability state, which was reflected in the lower RMT values acquired in the negative-peak condition compared to the positive peak. Furthermore, we systematically investigated the prevalence of μ-phase dependency of corticospinal excitability and found that 73% of all included subjects (all healthy right-handers) showed μ-rhythm phase dependency in both hemispheres (i.e., lower RMT in the negative-peak condition compared to the positive peak), while 84% and 80% of the subjects presented this effect in the motor-dominant and motor-non-dominant hemisphere, respectively. The findings of high prevalence of μ-phase dependency of corticospinal excitability among subjects, along with the evidence of a ubiquitous presence of this effect in the motor system at rest provide further arguments for the future potential of brain-state dependent EEG-TMS and therapeutic rTMS.

In the third paper (Stefanou et al., 2018), we investigated the role of phase synchronicity of μ-rhythm in interhemispheric communication between the primary motor cortices. To the best of our knowledge, no previous studies had examined to what extent interhemispheric communication can be predicted by phase-interactions of the pre-stimulus μ-oscillations in the human sensorimotor cortex. Moreover, most electrophysiological studies investigating interhemispheric M1-M1 interactions had, so far, disregarded the continuously fluctuating brain dynamics at the time of stimulation. In this study, we reported first findings from 16 healthy human subjects, in whom sIHI was investigated with dual-site millisecond-resolution brain-state dependent EEG-triggered TMS, based on the instantaneous pre-stimulus phase of μ-oscillations in the two primary motor cortices.

Our results showed that the high-excitable pre-stimulus in-phase condition, corresponding to synchronous EEG-negative peak of the endogenous μ-rhythm in both primary motor cortices, facilitates most efficiently the interhemispheric communication, leading to strongest sIHI. As noted previously, IHI relies significantly on transcallosal connections between reciprocal sites of the two M1 (Daskalakis et al., 2002). Animal studies prove that coordinated interhemispheric interactions majorly rely on transcallosal transfer, as in animals undergoing callosotomy interhemispheric synchronization is abolished (Engel et al., 1991). The transcallosal connections between reciprocal motor areas are predominantly mediated by excitatory axons, which cross the corpus callosum to act on local inhibitory neurons in the contralateral motor cortex (Daskalakis et al., 2002). Hence, we hypothesized that when a TMS pulse reaches the conditioning M1 at its high-

excitable state, during the negative peak of the endogenous μ-rhythm, it can induce (through transcallosal excitatory pathways) a domino-like transfer of maximal inhibition to the contralateral M1. The latter transfer should function optimally when the contralateral M1 is also in a highly-receptive (i.e., high-excitable) state, during the negative peak of the μ-rhythm.

Our findings corroborated this hypothesis, as we found that strongest sIHI was noted when both M1 were stimulated in the μ-rhythm negative peak condition. As previously discussed, these results are also in line with the theory of neuronal communication through coherence (Fries, 2005, Fries, 2015), indicating that temporal-binding at millisecond-scale of in-phase μ-oscillations may comprise an important mechanism for interhemispheric communication in the motor cortex. Conversely, the weakest sIHI occurred when the two M1 were out of phase and the conditioning M1 was in a low-excitability state (corresponding to the positive peak of the μ-rhythm).

To sum up, in this study we demonstrated that brain-state dependent EEG-TMS is a modality that enables highly-accurate studies of neuronal networks oscillations. Our findings indicate that temporal dynamics of oscillating reciprocal networks within the motor system affect decisively the large-scale interhemispheric network communication. Thus, future brain stimulation studies should regard the ongoing phase of brain oscillations, at the time of stimulation, in order to study or induce efficiently modulations of interhemispheric network interactions.

5. Synopsis

In the present thesis, we are concerned with the role of endogenous phase of sensorimotor μ-rhythm in modulating corticospinal excitability and interhemispheric communication between the primary motor cortices (M1) assessed by real-time electroencephalography-triggered transcranial magnetic stimulation.

In the first part, we present a custom millisecond-resolution electroencephalography (EEG) - triggered transcranial magnetic stimulation (TMS) system, which synchronizes TMS with specific phases of ongoing μ-oscillations over the two sensorimotor cortices. We show that the negative EEG deflection of the μ-rhythm corresponds to a higher cortical excitability state compared to the positive EEG deflection. We further show that real-time EEG-TMS may reduce the variability of TMS-induced corticospinal excitability effects, while we present the methodological pipeline for conduction of EEG-TMS experiments and discuss the technical requirements and future potential of EEG-TMS research.

In the second part of the thesis, we are concerned with the question of symmetry of μ-rhythm phase-dependency of corticospinal excitability using single-pulse EEG-TMS over the two primary motor cortices. Our results show no differences in the directionality or effect size of μ-phase dependency of corticospinal excitability of the two M1. Therefore, we suggest that the μ-oscillation phase-dependency of corticospinal excitability may be regarded as a ubiquitous physiological trait of the motor system at rest.

In the third part of the thesis, we are concerned with the role of endogenous phase of sensorimotor μ-rhythm in interhemispheric M1-M1 communication. We use short interval interhemispheric inhibition (sIHI) as measure of interhemispheric communication in a dual-coil real-time EEG-TMS experiment. Our findings show that strongest sIHI and thereby most effective interhemispheric communication occurs when both M1 are in-phase, while stimulated in the μ-rhythm negative peak condition. Thus, we conclude, in accordance with the theory of neuronal communication through coherence, that interhemispheric communication between the primary motor cortices is most effective when the reciprocal M1 neuronal networks oscillate in synchrony and are both at a high excitability state.

6. Zusammenfassung

In der vorliegenden Arbeit befassen wir uns mit der Rolle der endogenen Phase des sensomotorischen μ-Rhythmus in der Modulation der kortikospinalen Erregbarkeit und der interhemisphärischen Kommunikation zwischen den primären motorischen Kortizes (M1), die durch Echtzeit - Elektroenzephalographie (EEG) - ausgelöste transkranielle Magnetstimulation (TMS) untersucht werden.

Im ersten Teil präsentieren wir ein Echtzeit-EEG-TMS System mit Millisekundenauflösung, das TMS mit bestimmten Phasen endogener μ-Oszillationen über den beiden sensomotorischen Kortizes synchronisiert. Wir zeigen, dass die negative EEG-Ablenkung des μ-Rhythmus einem höheren kortikalen Erregbarkeitszustand im Vergleich zur positiven EEG-Ablenkung entspricht. Wir zeigen weiterhin, dass Echtzeit-EEG-TMS die Variabilität von TMS-induzierten kortikospinalen Erregbarkeitseffekten verringern kann, während wir die methodische Pipeline für die Durchführung von EEG-TMS-Experimenten vorstellen und die technischen Anforderungen und das zukünftige Potenzial der EEG-TMS-Forschung diskutieren.

Im zweiten Teil der Arbeit befassen wir uns mit der Frage der Symmetrie der μ-Rhythmus-Phasenabhängigkeit der kortikospinalen Erregbarkeit unter Verwendung von Einzelpuls-EEG-TMS über die beiden primären motorischen Kortizes. Unsere Ergebnisse zeigen keine Unterschiede in der Richtung oder Effektgröße der μ-Phasenabhängigkeit der kortikospinalen Erregbarkeit der beiden M1. Daher schließen wir daraus, dass die μ-Oszillationsphasenabhängigkeit der kortikospinalen Erregbarkeit als ein ubiquitäres physiologisches Merkmal des Motorsystems in Ruhe angesehen werden kann.

Im dritten Teil der Arbeit beschäftigen wir uns mit der Rolle der endogenen Phase des sensomotorischen μ-Rhythmus in der interhemisphärischen M1-M1-Kommunikation. Wir verwenden die interhemisphärische Inhibition mit kurzem Interstimulusintervall (sIHI) als Maß für die interhemisphärische Kommunikation in einem Echtzeit-EEG-TMS-Experiment mit zwei Spulen. Unsere Ergebnisse zeigen, dass die stärkste sIHI und damit die effektivste interhemisphärische Kommunikation auftritt, wenn beide M1 am negativen Peak des μ-Rhythmus stimuliert werden. In Übereinstimmung mit der Theorie der neuronalen Kommunikation durch Kohärenz schließen wir daher, dass die interhemisphärische Kommunikation zwischen den primären motorischen Kortizes am effektivsten ist, wenn die reziproken neuronalen M1-Netzwerke synchron oszillieren und sich beide in einem Zustand hoher Erregbarkeit befinden.

7. References

AMUNTS, K., JANCKE, L., MOHLBERG, H., STEINMETZ, H. & ZILLES, K. 2000. Interhemispheric asymmetry of the human motor cortex related to handedness and gender. *Neuropsychologia,* 38**,** 304-12.

ASANUMA, H. & OKUDA, O. 1962. Effects of transcallosal volleys on pyramidal tract cell activity of cat. *J Neurophysiol,* 25**,** 198-208.

BERGER, B., MINARIK, T., LIUZZI, G., HUMMEL, F. C. & SAUSENG, P. 2014. EEG oscillatory phase-dependent markers of corticospinal excitability in the resting brain. *Biomed Res Int,* 2014**,** 936096.

CHANG, H. T. 1953. Cortical response to activity of callosal neurons. *J Neurophysiol,* 16**,** 117-31.

DASKALAKIS, Z. J., CHRISTENSEN, B. K., FITZGERALD, P. B., ROSHAN, L. & CHEN, R. 2002. The mechanisms of interhemispheric inhibition in the human motor cortex. *J Physiol,* 543**,** 317-26.

DUBOVIK, S., PIGNAT, J. M., PTAK, R., ABOULAFIA, T., ALLET, L., GILLABERT, N., MAGNIN, C., ALBERT, F., MOMJIAN-MAYOR, I., NAHUM, L., LASCANO, A. M., MICHEL, C. M., SCHNIDER, A. & GUGGISBERG, A. G. 2012. The behavioral significance of coherent resting-state oscillations after stroke. *Neuroimage,* 61**,** 249-57.

ENGEL, A. K., KONIG, P., KREITER, A. K. & SINGER, W. 1991. Interhemispheric synchronization of oscillatory neuronal responses in cat visual cortex. *Science,* 252**,** 1177-9.

ENGEL, A. K. & SINGER, W. 2001. Temporal binding and the neural correlates of sensory awareness. *Trends Cogn Sci,* 5**,** 16-25.

FERBERT, A., PRIORI, A., ROTHWELL, J. C., DAY, B. L., COLEBATCH, J. G. & MARSDEN, C. D. 1992. Interhemispheric inhibition of the human motor cortex. *J Physiol,* 453**,** 525-46.

FRIES, P. 2005. A mechanism for cognitive dynamics: neuronal communication through neuronal coherence. *Trends Cogn Sci,* 9**,** 474-80.

FRIES, P. 2015. Rhythms for Cognition: Communication through Coherence. *Neuron,* 88**,** 220-35.

GEORGOPOULOS, A. P., KETTNER, R. E. & SCHWARTZ, A. B. 1988. Primate motor cortex and free arm movements to visual targets in three-dimensional space. II. Coding of the direction of movement by a neuronal population. *J Neurosci,* 8**,** 2928-37.

HAEGENS, S., HANDEL, B. F. & JENSEN, O. 2011a. Top-down controlled alpha band activity in somatosensory areas determines behavioral performance in a discrimination task. *J Neurosci,* 31**,** 5197-204.

HAEGENS, S., NACHER, V., LUNA, R., ROMO, R. & JENSEN, O. 2011b. alpha-Oscillations in the monkey sensorimotor network influence discrimination performance by rhythmical inhibition of neuronal spiking. *Proc Natl Acad Sci U S A,* 108**,** 19377-82.

HALLETT, M. 2007. Transcranial magnetic stimulation: a primer. *Neuron,* 55**,** 187-99.

HUBERS, A., OREKHOV, Y. & ZIEMANN, U. 2008. Interhemispheric motor inhibition: its role in controlling electromyographic mirror activity. *Eur J Neurosci,* 28**,** 364-71.

KLIMESCH, W., SAUSENG, P. & HANSLMAYR, S. 2007. EEG alpha oscillations: the inhibition-timing hypothesis. *Brain Res Rev,* 53**,** 63-88.

LECAS, J. C., REQUIN, J., ANGER, C. & VITTON, N. 1986. Changes in neuronal activity of the monkey precentral cortex during preparation for movement. *J Neurophysiol,* 56**,** 1680-702.

MIMA, T., OLUWATIMILEHIN, T., HIRAOKA, T. & HALLETT, M. 2001. Transient interhemispheric neuronal synchrony correlates with object recognition. *J Neurosci,* 21**,** 3942-8.

MUELLER, J. K., GRIGSBY, E. M., PREVOSTO, V., PETRAGLIA, F. W., 3RD, RAO, H., DENG, Z. D., PETERCHEV, A. V., SOMMER, M. A., EGNER, T., PLATT, M. L. & GRILL, W. M. 2014. Simultaneous transcranial magnetic stimulation and single-neuron recording in alert non-human primates. *Nat Neurosci,* 17**,** 1130-6.

MURTHY, V. N. & FETZ, E. E. 1996. Oscillatory activity in sensorimotor cortex of awake monkeys: synchronization of local field potentials and relation to behavior. *J Neurophysiol,* 76**,** 3949-67.

NICOLO, P., RIZK, S., MAGNIN, C., PIETRO, M. D., SCHNIDER, A. & GUGGISBERG, A. G. 2015. Coherent neural oscillations predict future motor and language improvement after stroke. *Brain,* 138**,** 3048-60.

PALVA, S. & PALVA, J. M. 2007. New vistas for alpha-frequency band oscillations. *Trends Neurosci,* 30**,** 150-8.

PFURTSCHELLER, G., STANCAK, A., JR. & NEUPER, C. 1996. Event-related synchronization (ERS) in the alpha band--an electrophysiological correlate of cortical idling: a review. *Int J Psychophysiol,* 24**,** 39-46.

RATHELOT, J. A. & STRICK, P. L. 2009. Subdivisions of primary motor cortex based on cortico-motoneuronal cells. *Proc Natl Acad Sci U S A,* 106**,** 918-23.

REIS, J., SWAYNE, O. B., VANDERMEEREN, Y., CAMUS, M., DIMYAN, M. A., HARRIS-LOVE, M., PEREZ, M. A., RAGERT, P., ROTHWELL, J. C. & COHEN, L. G. 2008. Contribution of transcranial magnetic stimulation to the understanding of cortical mechanisms involved in motor control. *J Physiol,* 586**,** 325-51.

RODRIGUEZ, E., GEORGE, N., LACHAUX, J. P., MARTINERIE, J., RENAULT, B. & VARELA, F. J. 1999. Perception's shadow: long-distance synchronization of human brain activity. *Nature,* 397**,** 430-3.

STEFANOU, M. I., BAUR, D., BELARDINELLI, P., BERGMANN, T. O., BLUM, C., GORDON, P. C., NIEMINEN, J. O., ZRENNER, B., ZIEMANN, U. & ZRENNER, C. 2019. Brain State-dependent Brain Stimulation with Real-time Electroencephalography-Triggered Transcranial Magnetic Stimulation. *J Vis Exp.*

STEFANOU, M. I., DESIDERI, D., BELARDINELLI, P., ZRENNER, C. & ZIEMANN, U. 2018. Phase Synchronicity of mu-Rhythm Determines Efficacy of Interhemispheric Communication Between Human Motor Cortices. *Journal of Neuroscience,* 38**,** 10525-10534.

STEFANOU, M. I., GALEVSKA, D., ZRENNER, C., ZIEMANN, U. & NIEMINEN, J. O. 2020. Interhemispheric symmetry of μ-rhythm phase-dependency of corticospinal excitability. *Sci Rep,* 10**,** 7853.

UGAWA, Y., HANAJIMA, R. & KANAZAWA, I. 1993. Interhemispheric facilitation of the hand area of the human motor cortex. *Neurosci Lett,* 160**,** 153-5.

VAN DER KNAAP, L. J. & VAN DER HAM, I. J. 2011. How does the corpus callosum mediate interhemispheric transfer? A review. *Behav Brain Res,* 223**,** 211-21.

VARELA, F., LACHAUX, J. P., RODRIGUEZ, E. & MARTINERIE, J. 2001. The brainweb: phase synchronization and large-scale integration. *Nat Rev Neurosci,* 2**,** 229-39.

WESTLAKE, K. P., HINKLEY, L. B., BUCCI, M., GUGGISBERG, A. G., BYL, N., FINDLAY, A. M., HENRY, R. G. & NAGARAJAN, S. S. 2012. Resting state alpha-band functional connectivity and recovery after stroke. *Exp Neurol,* 237**,** 160-9.

WOMELSDORF, T. & FRIES, P. 2006. Neuronal coherence during selective attentional processing and sensory-motor integration. *J Physiol Paris,* 100**,** 182-93.

YOKOI, A., ARBUCKLE, S. A. & DIEDRICHSEN, J. 2018. The Role of Human Primary Motor Cortex in the Production of Skilled Finger Sequences. *J Neurosci,* 38**,** 1430-1442.

ZRENNER, B., ZRENNER, C., GORDON, P. C., BELARDINELLI, P., MCDERMOTT, E. J., SOEKADAR, S. R., FALLGATTER, A. J., ZIEMANN, U. & MULLER-DAHLHAUS, F. 2020. Brain oscillation-synchronized stimulation of the left dorsolateral prefrontal cortex in depression using real-time EEG-triggered TMS. *Brain Stimul,* 13**,** 197-205.

ZRENNER, C., DESIDERI, D., BELARDINELLI, P. & ZIEMANN, U. 2018a. Real-time EEG-defined excitability states determine efficacy of TMS-induced plasticity in human motor cortex. *Brain Stimulation,* 11**,** 374-389.

ZRENNER, C., DESIDERI, D., BELARDINELLI, P. & ZIEMANN, U. 2018b. Real-time EEG-defined excitability states determine efficacy of TMS-induced plasticity in human motor cortex. *Brain Stimul,* 11**,** 374-389.

8. Author contributions

1. STEFANOU, M. I., BAUR, D., BELARDINELLI, P., BERGMANN, T. O., BLUM, C., GORDON, P. C., NIEMINEN, J. O., ZRENNER, B., ZIEMANN, U. & ZRENNER, C. 2019. Brain State-dependent Brain Stimulation with Real-time Electroencephalography-Triggered Transcranial Magnetic Stimulation. *J Vis Exp*.

M.-I.S., and C.Z. acquired the data, analysed/interpreted the data, and wrote the manuscript. D.B., P.B., T.O.B., C.B., P.C.G., J.O.N. and B.Z. critically reviewed the manuscript. U.Z. conceived the research, and critically reviewed the manuscript for important intellectual content. All authors read and approved the final manuscript.

2. STEFANOU, M. I., GALEVSKA, D., ZRENNER, C., ZIEMANN, U. & NIEMINEN, J. O. 2020. Interhemispheric symmetry of μ-rhythm phase-dependency of corticospinal excitability. *Sci Rep,* 10**,** 7853.

M.-I.S., D.G., C.Z., U.Z. and J.O.N. designed the experiment and data-analysis methods. **M.-I.S.,** D.G. and J.O.N. performed the experiments. **M.-I.S.** and J.O.N. analyzed the data. **M.-I.S.** and J.O.N. wrote the article. U.Z. revised the manuscript. All the authors reviewed the manuscript.

3. STEFANOU, M. I., DESIDERI, D., BELARDINELLI, P., ZRENNER, C. & ZIEMANN, U. 2018. Phase Synchronicity of mu-Rhythm Determines Efficacy of Interhemispheric Communication Between Human Motor Cortices. *Journal of Neuroscience,* 38**,** 10525-10534.

M.-I.S., D.D., P.B., and C.Z. wrote the first draft of the paper; U.Z. edited the paper; U.Z. designed research; **M.-I.S.,** D.D., P.B., and C.Z. performed research; **M.-I.S.,** D.D., P.B., C.Z., and U.Z. analyzed data; U.Z. wrote the paper.